

The Search for a Universal Tile

by
Feng Zhu

A Thesis
Submitted in partial fulfillment of
the requirements for the Degree of Bachelor of Arts with Honors
in Computer Science

Williams College
Williamstown, Massachusetts
May 20, 2002

Abstract

One of the most remarkable discoveries in the theory of tilings concerns the existence of sets of prototiles which admit infinitely many tilings of the plane without any of these tilings being periodic. Sets of prototiles with this property are called *aperiodic*. In 1966, R. Berger discovered a set of 20426 prototiles with corresponding matching rules to be aperiodic. Subsequently, the number of aperiodic prototiles was reduced to two by R. Penrose in 1974. It is still an open problem whether there is a single *universal* aperiodic two-dimensional prototile with corresponding matching rules.

In 1996, Gummelt identified a single decagon *covering* that *covered* the plane aperiodically. The covering allows tiles to overlap in five different ways. Our research is motivated by her approach. We seek to develop a partitioning of the regions such that points in different partitions never collide in an overlap. Such partitioning is achieved by a special coloring process which assigns each point to be one of the five colors. The coloring process is based on infinite decomposition of Robinson tiles and a Cantor-like construction. We will show that each color set has positive measure everywhere, that is, points in each color are dense enough to form area throughout the plane. Our approach will generate a non-traditional sponge-like tile.

Although we are able to convert Gummelt's decagon *covering* to decagon *tiling*, as the tile does not have a solid interior — the problem of finding a universal tile is still open.

Acknowledgments

“Do something. If it doesn’t work, do something else. No idea is too crazy.”

— Jim Hightower

I would like to thank my advisor, Duane Bailey, for everything he has done for me. His passion and intelligence impress me every day. Working with a professor like him has been my biggest reward in this project.

I also appreciate all the suggestions and corrections that came from Bill Lenhart and Cesar Silva, who reviewed my thesis in its various forms.

I am also very grateful to Colin Adams. Not only did he urge me to begin a thesis in the first place, but he also encouraged me through every stage of the process.

Last, but certainly not the least, I would like to thank Rossen Djagalov and Alan Velander for their moral support.

Contents

1	Introduction to Tilings	1
1.1	Tilings	1
1.2	Aperiodicity	2
1.3	Universal Tile	3
1.4	Inflation	6
1.5	Quasicrystals and Aperiodic Tilings	7
1.6	Summary	8
2	Recent Approaches to Finding a Universal Tile	9
2.1	Universal Decagon Covering	9
2.2	Penrose Tiles with Fractal Edges	12
2.3	Summary	15
3	A Method for Building Interleaved Point Sets	16
3.1	Construction for Our Simple Method	16
3.2	Measure	18
3.3	Analysis of Our Construction	19
3.4	Conclusion	20
4	The Decagonal Sponge Tile	21
4.1	Introduction	21
4.2	Construction	22
4.3	Analysis	27
	4.3.1 Measure	27
	4.3.2 Matching Rules	27
4.4	Conclusion	29

5	Second Construction of Color Sets	30
5.1	Introduction	30
5.2	1-D Color Sets	30
5.3	2-D Color Set Construction	33
5.3.1	Analysis	37
5.4	Our Decagonal Sponge Tile	41
5.4.1	Matching Rules of the Sponge Tile	42
5.4.2	Aperiodicity of the Sponge Tile	43
5.5	A Bin-Packing Approach	43
5.6	Conclusion	45
6	Conclusions and Future Work	46
6.1	Conclusions	46
6.2	Future Work	49
A	Cantor Set	50
B	Methods for Finding Fixed Points	51
B.1	Method 1: Play with Geometry	51
B.2	Method 2: Use Mapping Function	53
B.3	Summary	53
C	Postscript for Generating Fractal Tiles	54
D	Colophon	59

List of Figures

1.1	Penrose's kite and dart.	3
1.2	The Robinson's A tiles.	4
1.3	The Robinson's B tiles.	4
1.4	The Penrose Rhombs.	5
1.5	A tiling by Penrose Rhombs.	5
1.6	Inflation rule for Penrose's kite and dart.	6
1.7	Inflation rule for Robinson's large and small A tiles.	7
2.1	The zero-, first- and second-order cartwheels.	10
2.2	Gummelt's single aperiodic 'prototile' and its corresponding covering.	11
2.3	Possible overlaps of two decagons in Gummelt's decagon covering.	13
2.4	The transformation for generating fractal tiles.	14
2.5	The fractal tiles by Gummelt and Bandt.	15
3.1	The first few steps in our 1-D construction.	17
4.1	Regions in decagon distinguished by their relationship during tile overlaps.	22
4.2	The coloring of the various regions of the decagon tile.	24
4.3	Each color is associated with a portion of the kite or dart.	24
4.4	The first approximation to the coloring of the decagon tile.	25
4.5	A tiling formed by our first approximation.	26
4.6	Illegal ways to tile two decagon sponges.	28
5.1	The first few steps in generating a Cantor set of positive measure.	31
5.2	Address of the tile.	36
5.3	Our decagonal sponge tile.	42
5.4	A bin-packing algorithm for assigning color sets.	44
5.5	An illustration of our bin-packing algorithm.	44

6.1	Atomic decoration of the decagonal (2nm) quasi-unit cell for $\text{Al}_{72}\text{Ni}_{20}\text{Co}_8$.	47
6.2	Image of the high quality sample of $\text{Al}_{72}\text{Ni}_{20}\text{Co}_8$	48
A.1	An algorithm for generating the standard cantor set.	50
B.1	Right handed Robinson's A tile.	52

Chapter 1

Introduction to Tilings

Tilings surround us everywhere from bathroom tiles to bricks on a wall. We are on a search for a single tile — one that appears to tile the plane very irregularly. In fact, as we shall discover, there is great ‘regularity’ in many ‘irregular’ patterns. Before proceeding to discuss ‘irregularity’, we will give some formal definitions of *tiling* and relevant concepts.

1.1 Tilings

A **tiling** T is a countable family of closed sets $\{T_1, T_2, \dots\}$ which cover the plane without gaps or significant overlaps¹, i.e. the sets T_i are pairwise disjoint and their union forms the whole plane. An element of T is called a **tile**. We consider “the plane” as the Euclidean plane of elementary geometry.

When two tiles are of the same size and shape, we call them **congruent** to each other. For every tiling T there is a subset P such that no two tiles in P are congruent and every tile in T is congruent to a tile of P . The set P is called the **prototile** set of T . We say that P **admits** the tiling T .

A tiling has **translational symmetry** if the tiling can be shifted by a nonzero distance in some direction such that it matches itself exactly. Most of the tilings we come across everyday have this property. We say that they are periodic. Consequently, we call tilings that do not have translational symmetry non-periodic tilings. We will focus on a special subset of non-periodic tilings, aperiodic tilings, in the following chapters.

¹The tiles may overlap along their boundaries only.

Definition 1. *If no tilings admitted by a set of prototiles P are periodic, P is **aperiodic**.*

From the definition above, we know the essential feature of an aperiodic set of prototiles is that *every* tiling admitted by them is *necessarily* non-periodic.

1.2 Aperiodicity

A common method to generate a tiling is to cover the plane by placing copies of prototiles down edge-to-edge. We will look at a more systematic approach for certain tilings which is based on the idea of composition and self-similarity. A tiling T_1 is obtained by *composition* from a tiling T_2 if each tile of T_1 is a union of one or more tiles of T_2 . Naturally, we define *decomposition* as the reverse process of composition – the cutting up of a large tile into smaller ones.

Definition 2. *A tiling T with its prototiles P is **self-similar** if it has the following properties:*

- *A new set of prototiles P' can be formed by copies of tiles from P , i.e., each $P'_i \in P'$ is formed by k tiles of T with $k \geq 1$.*
- *There exists a mapping from P to P' with a fixed expansion factor $\tau \in \mathfrak{R}$, $\tau > 0$, $\tau \neq 1$, and this mapping is bijective.*

We call the process of increasing the size of self-similar tiles by expansion and then decomposing them into tiles of the original shape and size *inflation*.

Theorem 1. *A tiling is aperiodic if it is self-similar and the composition process is unique.*

*Proof*²: Suppose that there were such a translation t through a distance d . Then uniqueness of composition implies that t must also be a symmetry of every composed tiling. As we can obtain tilings with arbitrarily large tiles by repeated compositions. It is impossible for t to be a symmetry of tilings in which every tile contains a circular disk of diameter larger than d . We reach a contradiction, and the theorem is proved. \square

This theorem also indicates that an aperiodic tiling can be constructed through an inflation process. In fact, it is not known whether aperiodic sets of tiles can be constructed without inflation arguments.

²Simplified from [GS87], (p.524).

1.3 Universal Tile

The history of aperiodic tilings can be traced back to year 1966, in which R. Berger discovered the first aperiodic set of tiles with corresponding matching rules [Ber66]. The set consists of 20426 Wang tiles. Berger's remarkable discovery refuted Wang's conjecture in 1961 that no aperiodic set exists. It also motivated a number of mathematicians to look for aperiodic tilings with smaller number of prototiles. Berger himself was able to reduce his set of tiles to 104 shortly. In 1974, Sir Roger Penrose discovered a set of aperiodic prototiles which contains only two tiles. The tiles, which are named as *kite* and *dart* are shown in Figure 1.1. The sides are of two lengths in the ratio of $\tau : 1$, where $\tau = (1 + \sqrt{5})/2 = 1.618034 \dots$. This ratio is also known as the *golden ratio*. The matching rule is that we must put equal edges together and also match the colors at corresponding vertices.

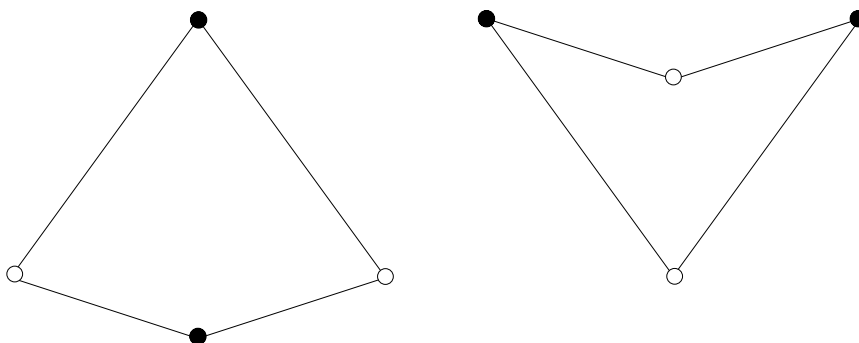


Figure 1.1: Penrose's kite and dart. The sides are of two lengths in the ratio $\tau : 1$. The angles are multiples of $\frac{\pi}{5}$ and the corners are colored with two colors (denoted by open and solid circles).

In 1975, Robinson proposed cutting each kite and dart into two triangles. In this way, we obtain the triangular 'A' tiles of Figure 1.2. The matching rule not only requires the same color at each vertex but also the same edge orientation. In Figure 1.3, we show how to compose Robinson's B tiles from the A tiles.

By alternatively grouping two similar Robinson's B tiles together, we obtain another aperiodic set of prototiles, named *Penrose rhombs*, shown in Figure 1.4. The matching rules of both Robinson's B tiles and Penrose rhombs are similar to those of the Robinson A tiles. An example of a tiling by these rhombs is shown in Figure 1.5.

The problem of whether there is a single *universal* aperiodic two-dimensional prototile with corresponding matching rules remains open.

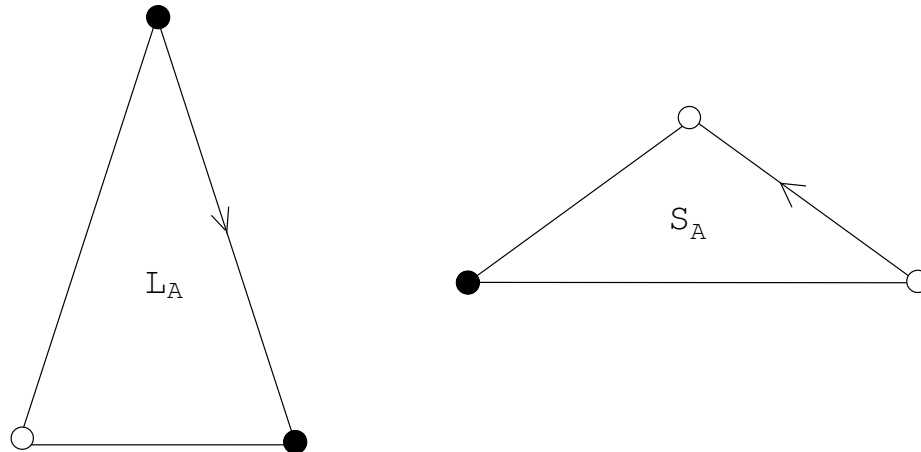


Figure 1.2: The larger and smaller tiles are denoted by L_A and S_A respectively. Two handed copies of each tile. Edge orientation is denoted by the arrows.

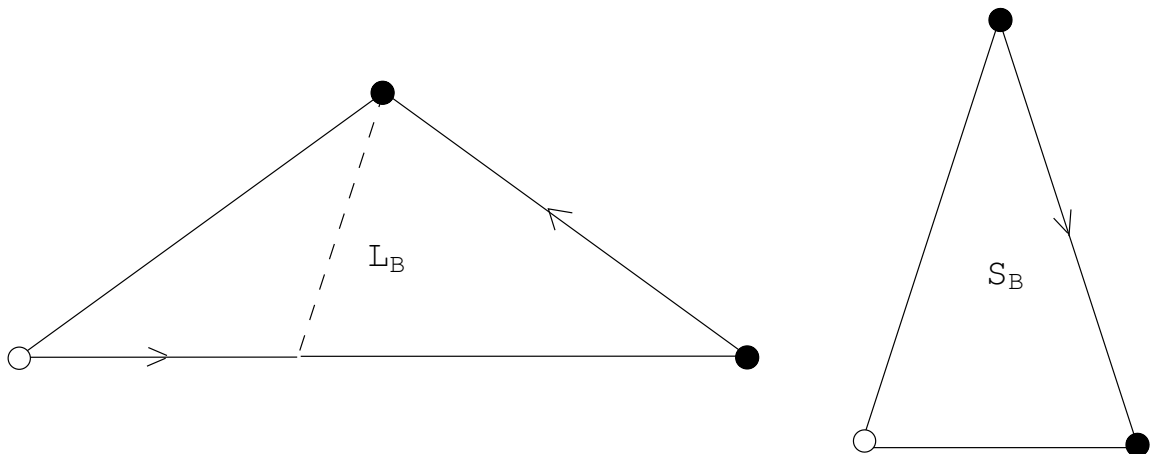


Figure 1.3: The larger and smaller tiles are denoted by L_B and S_B respectively. L_B is composed of one L_A and one L_B and S_B is the same as L_A .

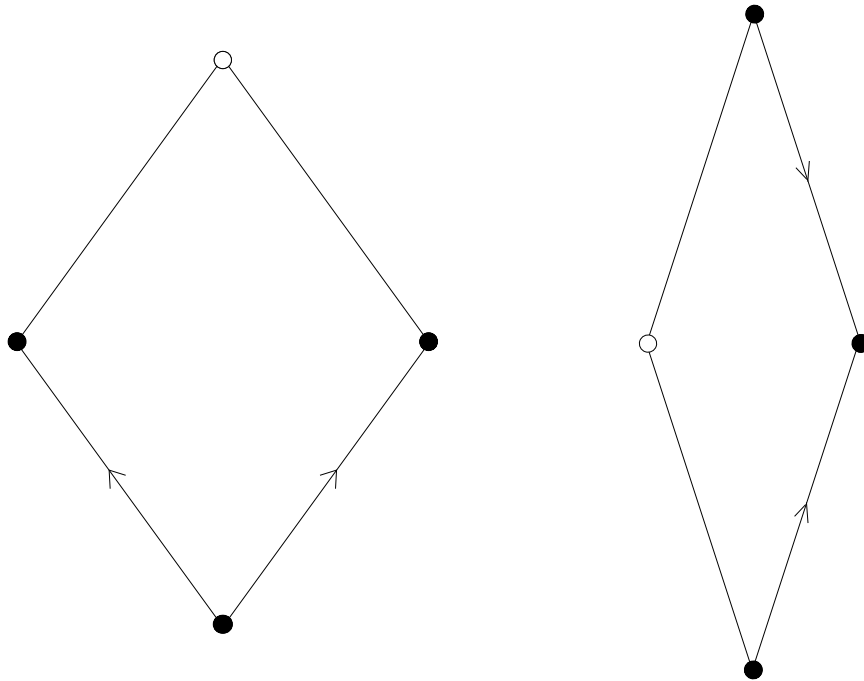


Figure 1.4: The Penrose Rhombs.

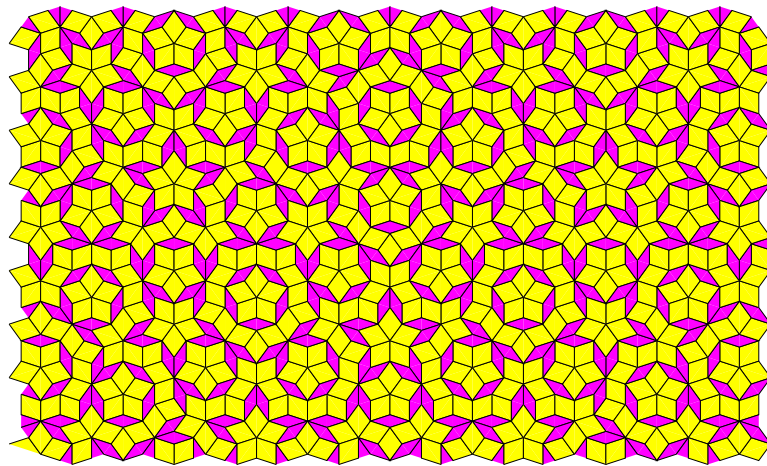


Figure 1.5: A tiling by Penrose Rhombs.

1.4 Inflation

In this section, we will take a look at how to inflate Penrose tiles and Robinson's A tiles. The inflation process requires that after we enlarge the tile by a fixed expansion factor, we should be able to tile it using our prototiles. The fixed expansion factor is τ for both Penrose tiles and Robinson's A tiles. Figure 1.6 illustrates the process of inflating the Penrose kite and dart. The matching rule ensures that the missing triangles (dashed) in the inflated kite are compensated by the two extra triangles (shaded) in the inflated dart. Since the composition process is unique, we can be assured that the missing components are available in neighboring regions.

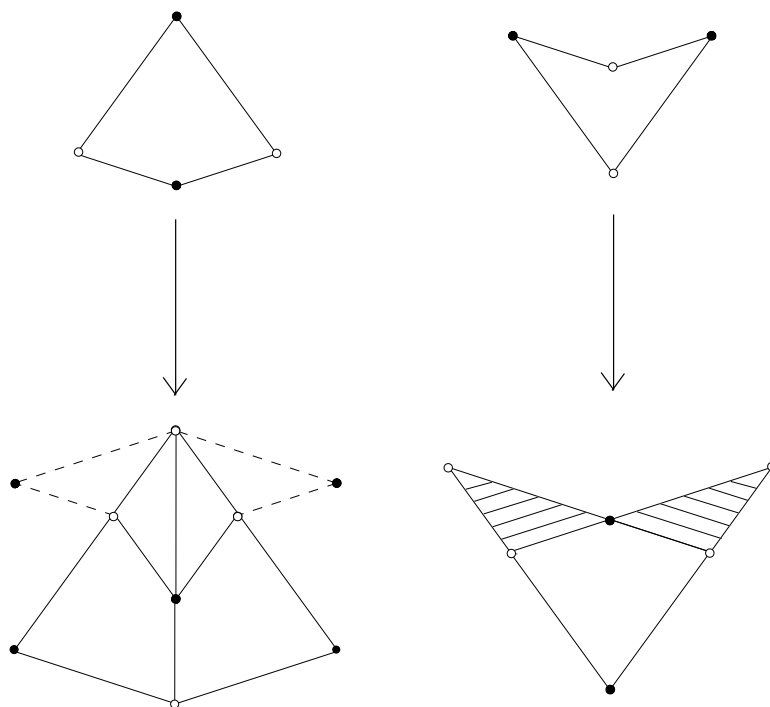


Figure 1.6: Inflation rule for Penrose's kite and dart.

During the inflation of Robinson's tiles, the new large A tile is composed of two large A tiles and one small A tile, while the new small A tile is composed by one large A tile and one small A tile. We illustrate the process in Figure 1.7. Notice that for both Penrose tiles and Robinson's tiles, the inflation processes interchange the colors

on the vertices.

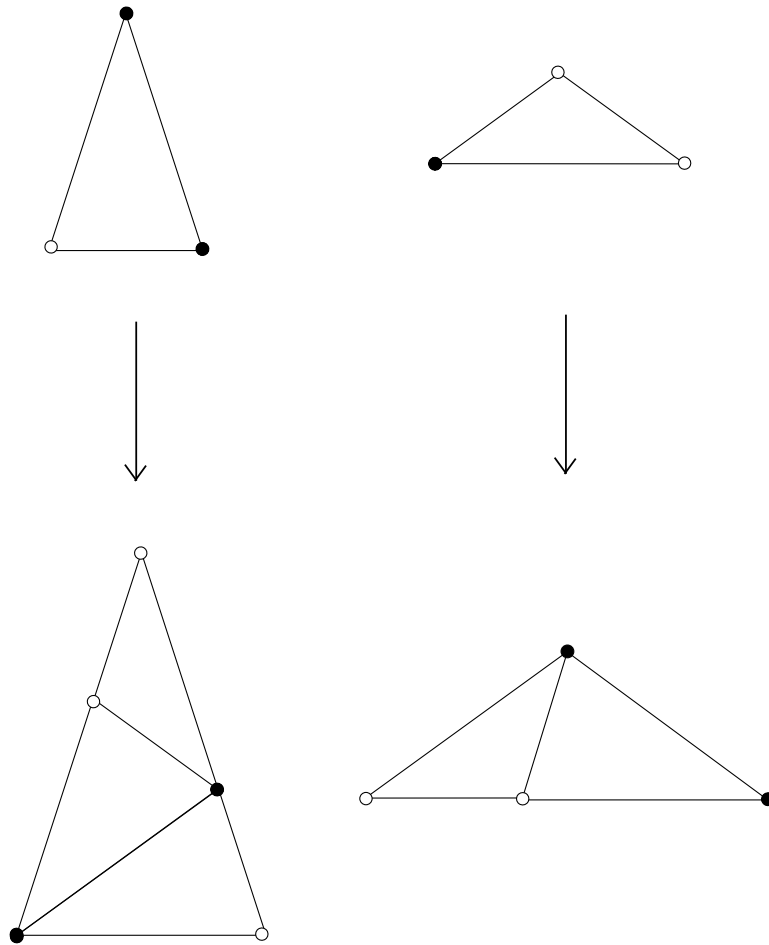


Figure 1.7: Inflation rule for Penrose's kite and dart.

If we scale the tiles back by the fixed expansion factor, the result is equivalent to the one after we decompose the original tile once.

1.5 Quasicrystals and Aperiodic Tilings

For hundreds of years, only two structural forms of solids were recognized: crystals, which are highly organized and based on a periodic building block called a unit cell,

and glasses, which have no periodic structure. In 1984, Shechtman, Blech, Gratias and Cahn [SBGC84] published a paper which marked the discovery of *quasicrystals*. They showed electron diffraction patterns of an Al-Mn alloy with sharp reflections and 10-fold symmetry. It is well-known that the only possible rotational symmetries resulting from periodicity are 2-, 3-, 4-, and 6-fold rotations. Five-fold rotations (and any n -fold rotation for $n > 6$) are incompatible with periodicity. The crystal Shechtman discovered, together with other similar crystals discovered since then, have been named *quasicrystals*. The Al-Mn alloy was classified as icosahedral quasicrystal that has 5-fold symmetry along one axis.

From the previous section, we have already seen an aperiodic tiling by using Penrose rhombs (Figure 1.5). An equivalent tiling in 3-D can be obtained by using rhombohedrons instead of rhombs. Shortly after the discovery of quasicrystals, a close resemblance was noted between the icosahedral quasicrystal and the 3D-Penrose pattern. In a similar way, 2D-Penrose rhombs can be used to form a decagon tiling approximating a decagonal quasicrystal that in a simple case consist of two layers with local 5-fold symmetry, which are rotated by 18 degrees so that the projection along the rotation axis gives a 10-fold symmetry. We will discuss decagon tiling in detail in the next chapter.

1.6 Summary

In this chapter, we provided many fundamentals about tilings. We are interested in aperiodic tilings, a particular subset of tilings, because the aperiodicity helps scientists understand quasicrystals, a new breed of strange high-tech materials. In particular, we discussed in detail Penrose tiles, the most famous example of an aperiodic set of tiles, and several of its variations. In the following chapters, we will look at two recent attempts at searching for universal tiles and then present our approaches.

Chapter 2

Recent Approaches to Finding a Universal Tile

In this chapter, we will take a look at two nonstandard tilings: Gummelt's aperiodic universal decagon **covering** and Penrose tiles with fractal boundaries.

2.1 Universal Decagon Covering

Before we discuss Gummelt's decagon covering, we shall take a brief look at a special tiling by Penrose kites and darts called *cartwheel tiling*. A cartwheel tiling can be constructed by inflating an *ace*, which consists of two kites and one dart (See Figure 2.1 (a)), an even number of times. We call a patch of a Penrose tiling is the n -th order cartwheel if it is constructed by inflating an ace $2n$ times. Figure 2.1 shows the first few cartwheels.

Gummelt shows in her paper that the Penrose tilings can also be generated by a single aperiodic 'prototile'. However, in contrast to *edge-to-edge* matching rules of common tiles, Gummelt also allows the copies of the prototile to intersect in sets with nonempty interior. Figure 2.2 shows the prototile she used and a corresponding covering. It is easy to see that the 'prototile' used here is a first-order cartwheel. Conway's theorem guarantees that such construction will be able to cover the whole plane:

Theorem 2. (Conway) *Every tiling by Penrose kites and darts can be covered by overlapping cartwheels.*

A proof of this can be found in Grünbaum and Sheppard [GS87], (p.562).

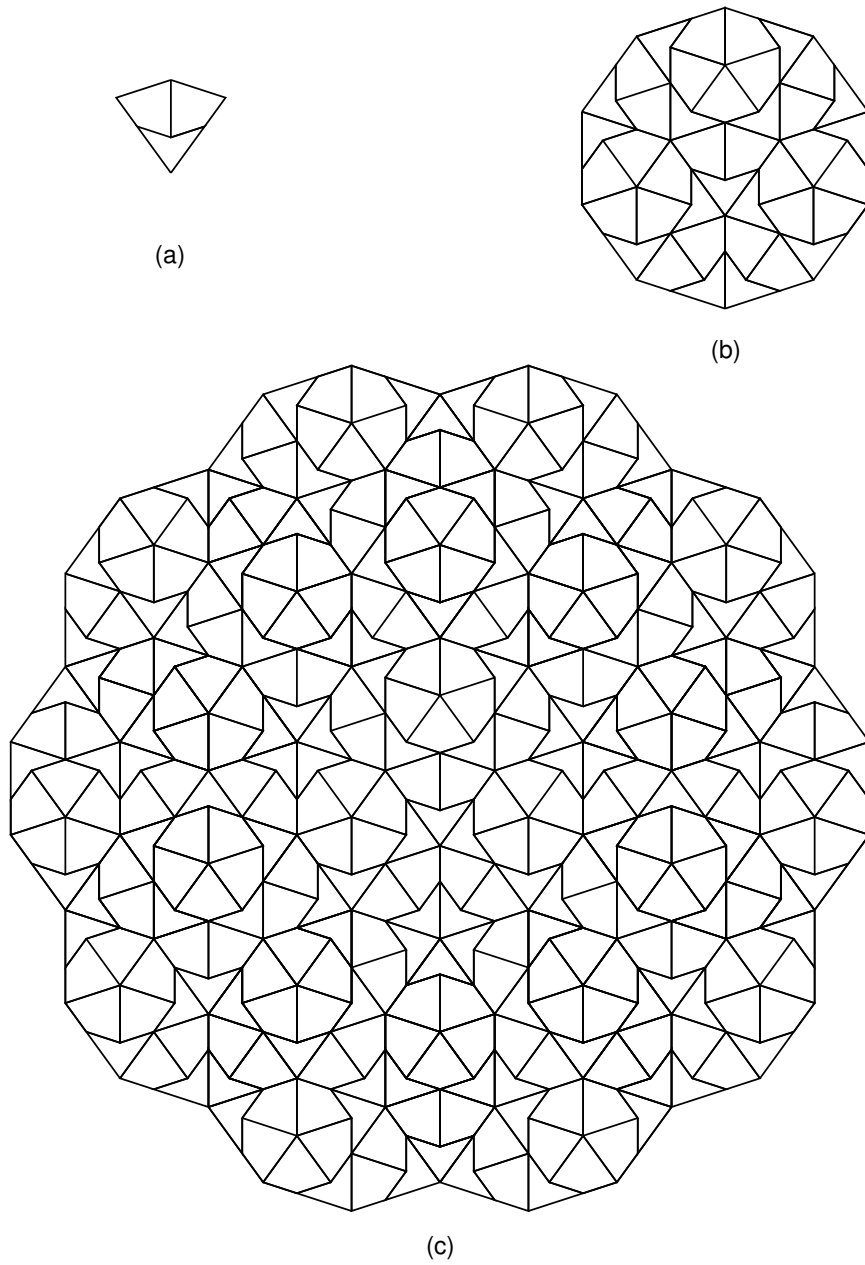


Figure 2.1: (a), (b), (c) are the zero-, first- and second-order cartwheels respectively. A few tiles are trimmed during the inflation process so that the resulting patches have the property that the union of the tiles in each patch is a polygon with symmetry group d_5 .

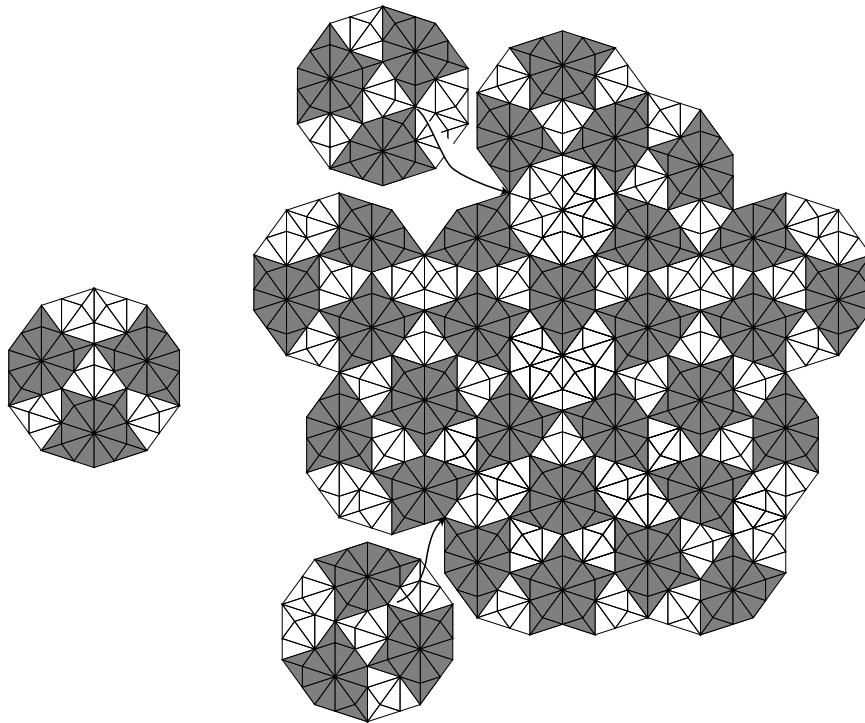


Figure 2.2: A single aperiodic ‘prototile’ and its corresponding covering. The arrows show how we use this prototile to cover (not tile) the plane. Note the five-fold symmetry of many of the subpatches of the covering.

In a perfect decagon covering of the plane, four types of intersection between any pair of cartwheels are allowed:

Case 1: The cartwheels do not intersect. This is the most common scenario.

Case 2: The cartwheels meet edge-to-edge, intersecting in an area of measure 0.

Case 3: The cartwheels overlap in an area which contains 4 darts and 7 kites (approximately 28.15% of the area of each of the participating cartwheels). Gummelt refers to such overlap as Type A.

Case 4: The cartwheels overlap in an area which contains 7 darts and 14 kites (approximately 54.46% of the area of each of the participating cartwheels). Gummelt refers to such overlap as Type B.

Figure 2.3 shows all possible A and B overlaps. Notice that there are four kinds of A-overlaps and one B-overlap. Just as most aperiodic tilings have matching rules, the decagon covering also has its *overlapping rule* that is based on the two types of overlaps.

OVERLAPPING RULE. *The dark subsets of every marked decagon D have to be overlapped by other tiles, such that the union of these pieces contains the boundary of D (∂D) and colors of overlapping sets are identical.*

In Gummelt's paper, she shows that the decagon is an a single aperiodic 'prototile'. The conclusion is reached by exhaustively examining possible neighborhoods for a cartwheel, given the overlapping rule. Details of the proof can be found in Gummelt's excellent paper [Gm96].

2.2 Penrose Tiles with Fractal Edges

One approach to construct a universal aperiodic prototile is to use fractal boundaries. In 1997, Gummelt and Bandt made such attempt. However, they were still unable to reduce the size of aperiodic prototile set to one. The result is an aperiodic prototile set of two tiles, each with fractal edges.

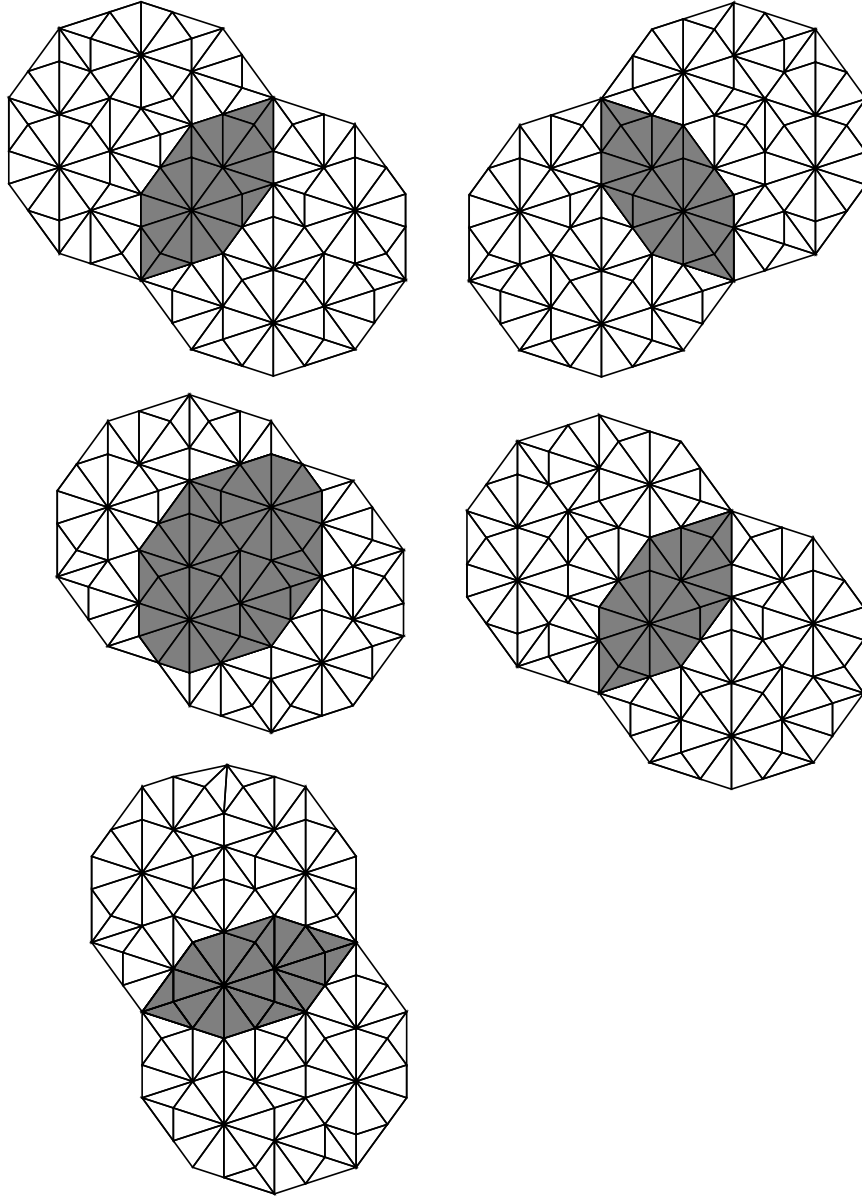


Figure 2.3: Possible overlaps of two decagons. The four smaller overlaps are called “A” overlaps and the larger region a “B” overlap.

The two tiles are generated based on the Penrose kite and dart. First, two transformations, as shown in Figure 2.4, are established for the kite and dart. Then the

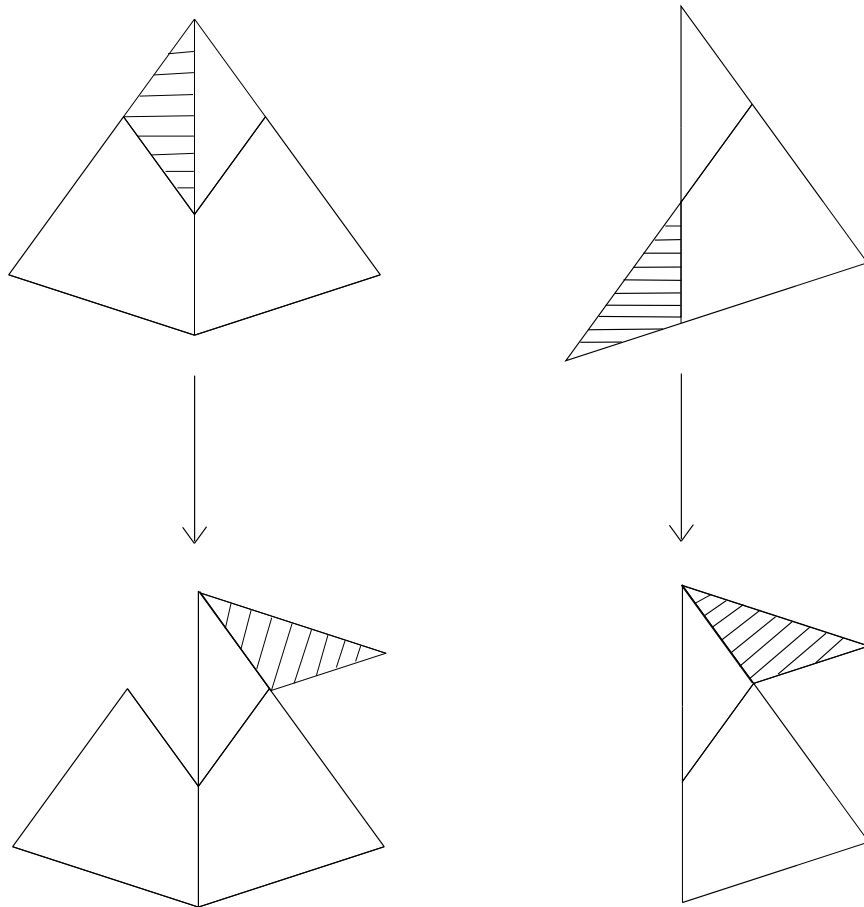


Figure 2.4: The transformation for generating fractal tiles. Essentially, the transformation places the shaded areas into new positions as shown.

following algorithm is applied for both kite and dart to generate the two fractal tiles.

```

while(true) {
    perform transformations for kites and darts if any
    perform inflation procedures on kites and darts
}
    
```

The two fractal tiles are shown in Figure 2.5. It has been proved by G. Gelbrich that the tiling admitted by the two fractal tiles are equivalent to the ordinary Penrose tilings.

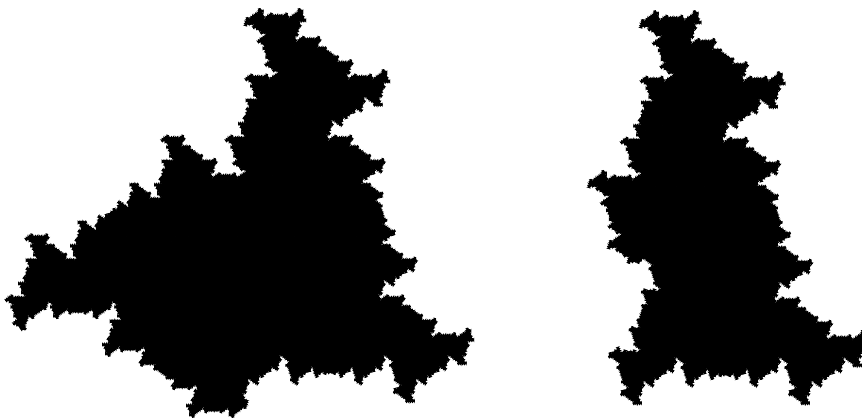


Figure 2.5: The fractal tiles by Gummelt and Bandt.

The unique characteristic of the fractal tiles is that matching rules are no longer needed to enforce the aperiodicity. The fractal boundaries provides perfect matching rules.

2.3 Summary

While the idea of a universal aperiodic prototile is appealing, no such prototile has been found. The difficulty lies in the fact that there is no mechanism to generate aperiodic prototiles. Although unsuccessful, the two recent approaches provide us with some ideas on how to search for such a universal tile. Both approaches are non-traditional and break some rules. The decagon covering allows the tile to overlap in a controlled manner, while the fractal approach generates tiles with fractal boundaries. One possible way to search for a universal tile is to take the result of these approaches and try to eliminate these “illegal” parts.

Chapter 3

A Method for Building Interleaved Point Sets

We shall, at times, have need for several sets of points or *colors* that are interleaved, or intermingling. We describe here a simple mechanism for defining these sets.

3.1 Construction for Our Simple Method

In this chapter, we will consider a simple example to illustrate the property of our coloring-scheme. We will construct three color sets in 1-D space.

Let $F_0 = [0, 1]$ and color set $C = \{Red, Green, Black\}$. In the zero-th step, we divide F_0 into three intervals $R_0 = (0, \frac{1}{3})$, $G_0 = (\frac{1}{3}, \frac{2}{3})$ and $G'_0 = (\frac{2}{3}, 1)$. We assign Red color to all the points in R_0 and Green color to all the points in G_0 and G'_0 .

We perform the following operations repeatedly to divide each interval into sub-intervals:

- For each $R_i = (a, b)$, we divide the interval into $G_{i+1} = (a, a + \frac{(b-a)}{3})$, $R_{i+1} = (a + \frac{(b-a)}{3}, a + \frac{2(b-a)}{3})$ and $G'_{i+1} = (a + \frac{2(b-a)}{3}, b)$.
- For each $G_i = (a, b)$ or $G'_i = (a, b)$, we divide the interval into $R_{i+1} = (a, a + \frac{(b-a)}{3})$, $G_{i+1} = (a + \frac{(b-a)}{3}, a + \frac{2(b-a)}{3})$ and $G'_{i+1} = (a + \frac{2(b-a)}{3}, b)$.
- A point $p \in F_0$ has color c in step i ($i \geq 0$), where

$$c = \begin{cases} \text{Red}, & \text{when } p \in R_i \\ \text{Green}, & \text{when } p \in G_i \text{ or } p \in G'_i \\ \text{Black}, & \text{otherwise} \end{cases}$$

Figure 3.1 illustrates the first few steps. (Black points are not shown.) Notice that, at each step, red and green points can be found spread fairly uniformly throughout the interval. While in a standard *Cantor set*¹, points kept and removed are distributed non-uniformly.

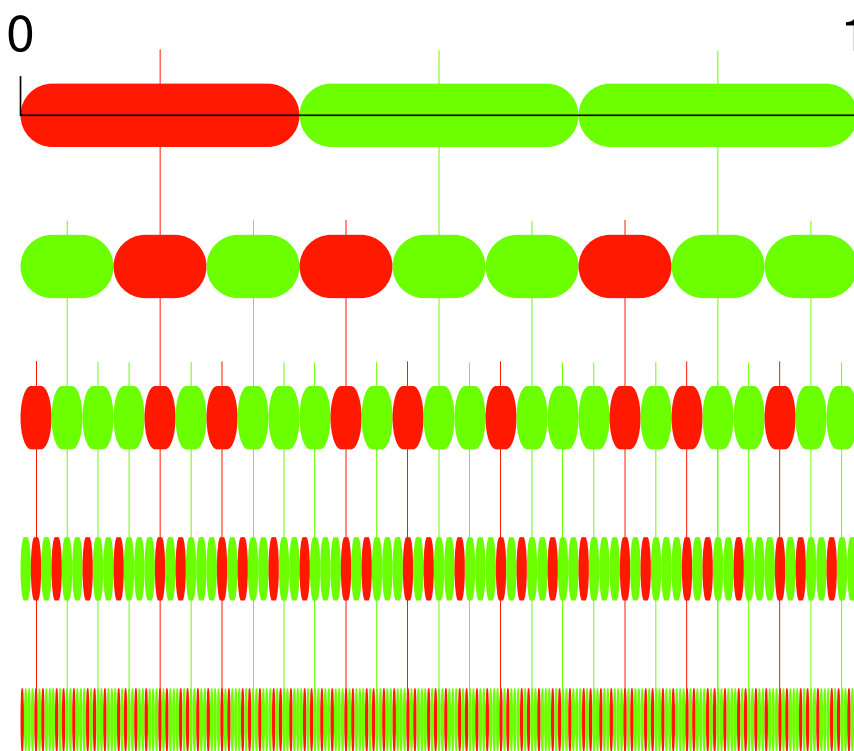


Figure 3.1: The first few steps in our construction. Black points are boundary points, and not shown. We note that there is no reflective symmetry of the points of this set. (Consider the points $(\frac{1}{6}, 0)$ and $(\frac{5}{6}, 0)$.)

Each point in F_0 has a *color sequence*. For instance, the point $(\frac{1}{2}, 0)$ has its color sequence $\{G, G, G, \dots\}$; the point $(\frac{1}{54}, 0)$ has its color sequence $\{R, G, R, G, G, G, \dots\}$.

¹For a description about Cantor set, please see Appendix A.

Definition 3. If the color sequence of point $p \in [0, 1]$ ultimately agrees term by term with $\{c, c, c, \dots\}$, where $c \in C$, that is, the color sequence contains a finite number of non- c terms, we define **the color of a point p** to be c . Otherwise, we define **the color of a point p** to be

$$c = \begin{cases} \text{Red}, & \text{when } p \in R_0 \\ \text{Green}, & \text{when } p \in (G_0 \cup G'_0) \end{cases}$$

3.2 Measure

In this section we introduce some basic concepts of measure theory needed for our constructions.

A measure is a means of assigning a number μ to certain subsets of a space. Measures are widely used in various fields of mathematics. Among different types of measures, we are interested in *Lebesgue measure*, which is used to analyze the Euclidean spaces \mathfrak{R}^d for $d \geq 1$.

Lebesgue measure in \mathfrak{R}^1 generalizes the notion of length. The Lebesgue measure of any interval is its length. A positive measure implies the set of points are dense enough to constitute some length, such as the set of all irrationals in $[0, 1]$. A zero measure implies points accumulate to nothing much, such as rationals in $[0, 1]$. The measure of a set in \mathfrak{R}^1 is the measure of a minimal cover of the set by open intervals.

Similarly, a positive Lebesgue measure in \mathfrak{R}^2 implies the set of points are dense enough to constitute some “area.” The measure of a set in \mathfrak{R}^2 is the area of a minimal cover of the set by, say, open circular discs. Sponges and many fractals have positive measures. Line segments have zero measure in \mathfrak{R}^2 .

We will use $\mu(S)$ to denote the measure of set S .

From measure-theoretic point of view, a tiling is a union of closed measure positive sets which cover the plane without any measure positive overlaps.

The following two lemmas are frequently used when we analyze the measure of some set.

Lemma 1. *If a set S is countable, then S has measure 0.*

Proof: We need to show that given any ϵ , we can cover S with a countable number of intervals such that the sum of the length of these intervals is less than ϵ .

Assume $S = \{a_1, a_2, a_3, \dots, a_i, \dots\}$. We put a disk of diameter $\frac{\epsilon}{2^{(i+1)}}$ around a_i . Therefore, we have an infinite number of intervals whose length are $\frac{\epsilon}{4}, \frac{\epsilon}{8}, \frac{\epsilon}{16}, \frac{\epsilon}{32}, \dots$ and they cover the set S .

It is easy to see that the sum of those infinite intervals is $\frac{\epsilon}{2} < \epsilon$, and the lemma is proved. \square

Lemma 2. *The measure of a countable set of pairwise disjoint measurable sets is the sum of the measure of each set.*

For proof, see Chapter 2, Silva [Sil02]. \square

3.3 Analysis of Our Construction

We now return to our construction in the previous section and consider the following three questions:

1. What is the measure of the set containing all the Black points?

At step n , let set G be the union of all open intervals and K be the set containing all the Black points. Since $K = F_0 \cap G^c$, K is closed. Furthermore, K and G are measurable and when $n \rightarrow +\infty$

$$\mu(G) = \lim_{n \rightarrow \infty} 3^{n+1} \times \frac{1}{3^{n+1}} = 1$$

Since $K \cup G = [0, 1]$, by Lemma 2, $\mu(K) = 1 - \mu(G) = 0$. Thus K has measure 0. \square

2. What is the measure of the set containing all the Red points?

According to Lemma 2, we have $\mu(\text{the set of all Red points}) + \mu(\text{the set of all Green points}) + \mu(\text{the set of all Black points}) = 1$. Also in each step, the measure of the red points is $1/2$ the measure of the green points. Since $\mu(\text{the set of all Black points}) = 0$, $\mu(\text{the set of all Red points}) = \frac{1}{3}$. \square

3. What is the measure of the set S , where a point p with color c is in S if and only if the color sequence of p contains finite number non- c terms?

Consider Red points first. The set of Red points whose color sequences end with all R's are countable. Similarly, the set of Green points whose color sequences end with all G's are countable. Thus, their union is countable. According to Lemma 1, the union has measure 0. Since all the Black points will have their color sequence end with (B, B, B, \dots) and the set of Black points has measure 0, the set which contains all points with their color sequence end with same color has measure 0. \square

The difficulty with our construction of red and green points is that a great number of points — indeed almost all of them — change color an infinite number of times during the construction process. So, while at each stage of the construction, $1/3$ of the points are red and $2/3$ are green, the red and green points move about sufficiently to make it a poor means of defining — in the limit — two sets of interleaved points that have measure > 0 . We will seek better methods for defining these sets including an improved coloring of the unit interval in Chapter 5. The focus in the next chapter is to define a better decomposition of the regions.

3.4 Conclusion

In this chapter, we attempted to develop two collections of points that interleave perfectly and have positive measures. In the next chapter, we will see how to construct such sets in 2-D — they are stepping stones to constructing non-overlapping tiles that share the same space. We seek a method of recursively defining regions that makes it possible to establish disjoint sets of points that are dense in the interval and also measure positive.

Chapter 4

The Decagonal Sponge Tile

The work of Gummelt has much promise in modelling real-world quasicrystals. In this chapter, we analyze the interactions a single decagon tile — a tile that may push us closer to establishing the status of the universal tile.

4.1 Introduction

In this chapter, we will construct a decagonal sponge tile. The decagonal sponge tile will have the following properties:

1. It tiles the whole plane aperiodically, similar to Gummelt's decagonal covering. (Figure 2.2)
2. The tile is a decagon-bounded collection of Cantor-like sets. Each set does not have solid interior. Instead, interior regions are constructed from Cantor-like sponges.
3. When the tiles interact with each other to form a tiling based on Gummelt's A-type or B-type overlapping, no points will collide with each other. In addition, each region will have positive measure.

You might have already noticed from the three properties above that the decagonal sponge tile we are developing is a non-traditional tile. Essentially we are seeking a way to convert Gummelt's *covering* into a *tiling* by partitioning regions into disjoint sets of points.

4.2 Construction

The overlapped regions in Gummelt’s covering are our main focus. Therefore, we begin our construction by identifying regions which act similarly during any of the five different overlaps (recall Figure 2.3). These regions are depicted in Figure 4.1. Such a partition helps to guide the selection of disjoint sets of points that will allow the tiles to “overlap” by interleaving.

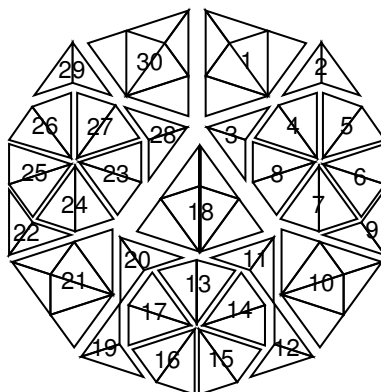


Figure 4.1: The various regions can be distinguished by their relationship during tile overlaps.

Based on our partition, we can summarize all associations of regions under each of the five overlaps in Table 4.1.

In order to satisfy property 3, we need to guarantee that if two regions are mapped to one another by an overlap, they must not contain coincident points. Thus in our second step, we try to develop a partitioning or *coloring* of the regions such that similarly colored regions never meet in an overlap. Theoretically, n color sets, where $n \geq 5$ (a minimum of 5 colors are required due to the relations of “sun”¹ patterns in overlaps), can meet this requirement. We find 5 color sets provide a suitable result, as shown in Table 4.2. The resulting 5-colored decagon is demonstrated in Figure 4.2.

It remains to develop tile shapes that (1) cover the indicated regions when no overlap occurs in that region, and (2) allow the joint covering of the indicated regions when overlap does occur. It is difficult to see how a single shape can accomplish both tasks. Our approach, however, is to develop independent sets of points with positive

¹A sun consists of five kites at its center.

$A_1 \leftrightarrow A_3$	$A_1 \leftrightarrow A_4$	$A_2 \leftrightarrow A_3$	$A_2 \leftrightarrow A_4$	$B_1 \leftrightarrow B_2$
1 ↔ 21	1 ↔ 30	10 ↔ 21	10 ↔ 30	3 ↔ 22
2 ↔ 20	2 ↔ 28	11 ↔ 19	11 ↔ 29	4 ↔ 25
3 ↔ 19	3 ↔ 29	12 ↔ 20	12 ↔ 28	5 ↔ 26
4 ↔ 17	4 ↔ 27	13 ↔ 16	13 ↔ 26	6 ↔ 27
5 ↔ 13	5 ↔ 23	14 ↔ 17	14 ↔ 27	7 ↔ 23
6 ↔ 14	6 ↔ 24	15 ↔ 13	15 ↔ 23	8 ↔ 24
7 ↔ 15	7 ↔ 25	16 ↔ 14	16 ↔ 24	9 ↔ 28
8 ↔ 16	8 ↔ 26	17 ↔ 15	17 ↔ 25	10 ↔ 18
9 ↔ 12	9 ↔ 22	19 ↔ 12	19 ↔ 22	11 ↔ 20
				12 ↔ 11
				13 ↔ 17
				14 ↔ 13
				15 ↔ 14
				16 ↔ 15
				17 ↔ 16
				18 ↔ 21
				20 ↔ 19

Table 4.1: The association of regions under each of the 5 different overlaps. Left regions appear in one tile, right regions appear in the other tile.

Color:	Green	Red	Purple	Yellow	Orange
Regions:	1	7	8	4	5
	2	14	15	10	17
	3	20	19	12	18
	6	22	21	16	24
	9	26	27	23	
	11	28			
	13	29			
	25	30			

Table 4.2: The partitioning of regions into five colors. When two regions are matched in Table 4.1, they have different colors. Their coloring is minimum due to the relations of “sun” patterns in overlaps.

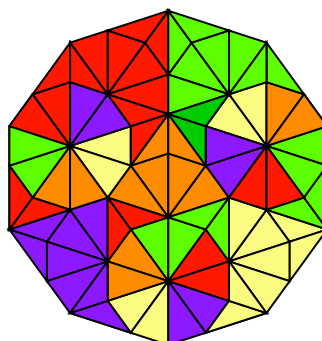


Figure 4.2: The coloring of the various regions of the decagon tile. If two regions can overlap they are guaranteed to have different colors.

measure that are dense in the specified regions. Each region “color” essentially translates to a two-dimensional sponge that has sufficient porousness to allow the overlap of differently colored sponges.

Analogously to our 1-D example in Chapter 3, we will use a decomposition process to classify points within a patch of tiles. As we have mentioned before, we need a minimum of five colors to classify points. Therefore, we first associate each of the five colors with a portion of the kite or dart, as shown in Figure 4.3.

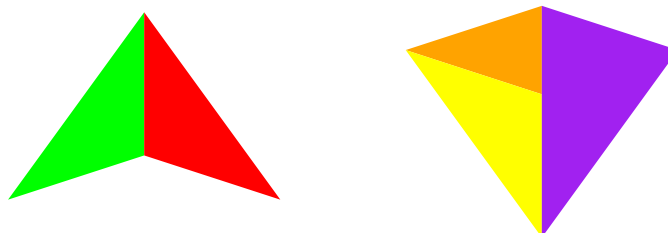


Figure 4.3: Each color (Green, Red, Orange, Yellow or Purple) is associated with a portion of the kite or dart. Because we need five colors, we decompose half of the kite into a smaller kite and dart.

The process of assigning points a particular “color” is similar to 1-D case and it involves generating the sequence of colors for that point at each stage in the decomposition process. For example, a point is colored green during iteration i if the point unambiguously resides in the interior of the right side of a dart. If a point is colored

c in all but a finite number of points during the decomposition process, we assign the point color c . Otherwise, we will assign the first color in its color sequence to be its color. All the boundary points will be marked black.

Once every point in the decagon has been assigned a color, for each region in Figure 4.2, we only keep points of the same color as the region. The first approximation to the coloring of the decagon tile, i.e. the result we obtain after one decomposition, is shown in Figure 4.4.

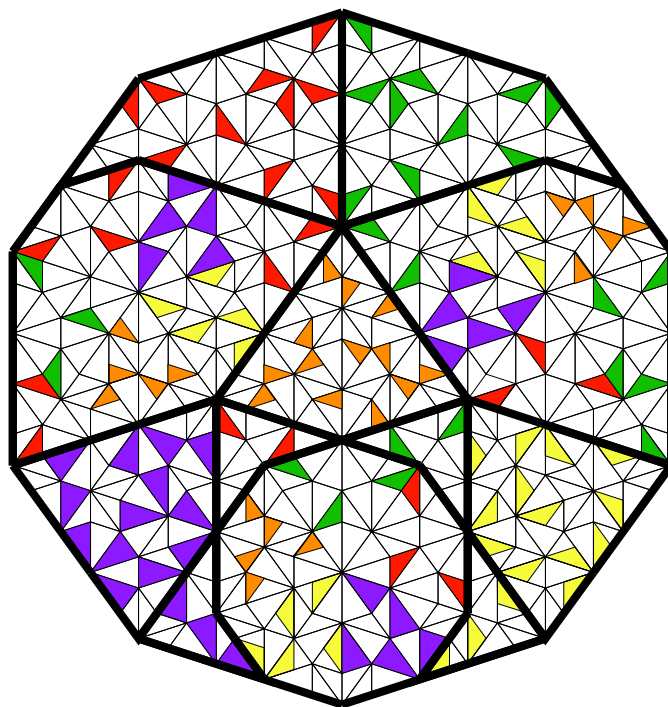


Figure 4.4: The first approximation to the coloring of the decagon tile. Dark boundaries are interior or exterior edges.

An approximation to our sponge tiling can be generated by using the first approximation to the coloring of the decagon tile. We show it in Figure 4.5.

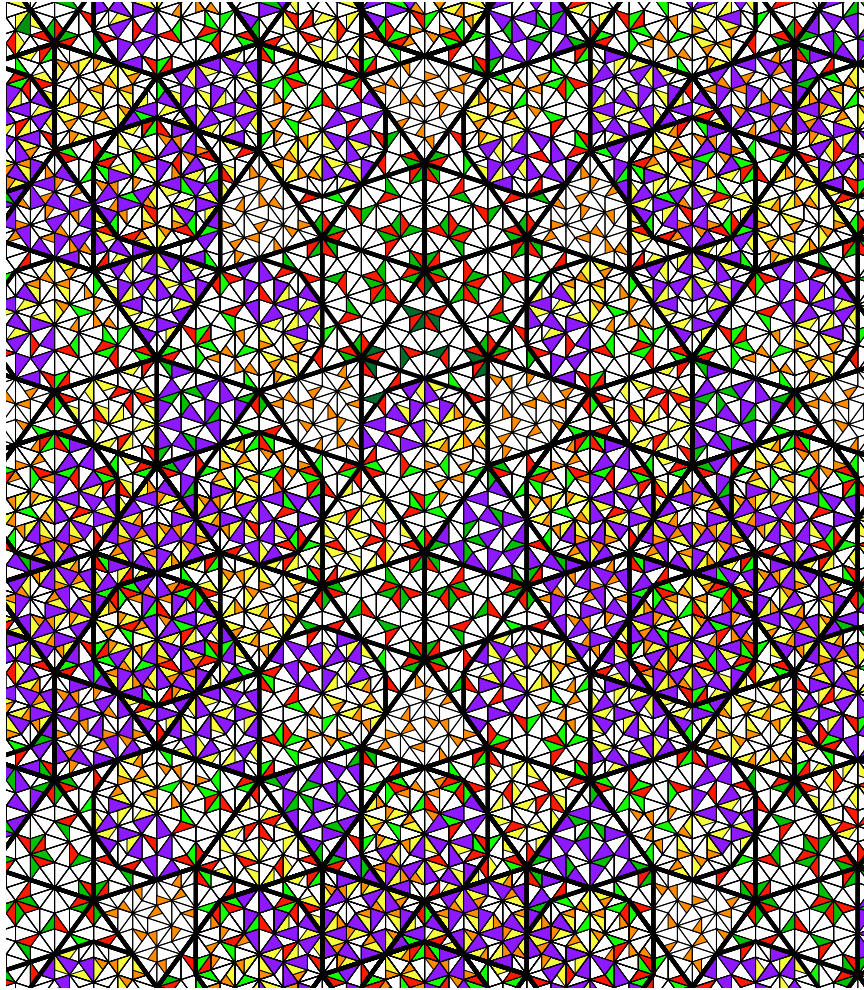


Figure 4.5: A tiling formed by our first approximation.

4.3 Analysis

4.3.1 Measure

Based on our 1-D analysis, we are able to make the conjecture that the measure of all points with color c , where $c = \text{Red, Green, Yellow, Orange or Purple}$, is positive. Also the positive measure depends on the indecisive points, i.e., the points we colored using the first terms in their color sequences. Therefore, points with certain color c are dense only within a fixed region, i.e., the region with color c initially, although they are everywhere throughout the tile. Such construction is not satisfactory for the sponge to be a cover, we would like it to have the meaning of an “area” everywhere. That is, we would like it to have positive measure for any color in every open ball.

4.3.2 Matching Rules

In Gummelt’s decagon covering, she also allows one decagon, T_1 , to tile with some other decagon, T_2 , edge-to-edge. That is, T_1 and T_2 do not overlap. However, whenever we have this situation, we can always add a decagon T_3 on top of T_1 and T_2 such that T_3 overlaps with both T_1 and T_2 in one of the five ways defined in Figure 2.3. In fact, after we tile the whole plane, adding T_3 or not will not change the tiling as every region in T_3 will overlap with some existing tiles. Therefore, Gummelt’s decagon overlapping rule also implies that in the decagonal covering, every external edge must be covered by some edge internal to the tile. Combined with our coloring scheme, we define our matching rules for the sponge tiling as:

Matching Rules

1. Every external edge is covered by one or more internal edges.
2. No region (in terms of Figure 4.1) can be tiled by more than one sponge with a given color.

Our matching rules essentially ensure that two interleaved sponges can only tile in the same way as one of the five possible decagon overlaps. In Figure 4.6, we present some possible illegal ways to tile two decagon sponges. It is easy to see all of them violate the second matching rule. In the next Chapter, we will see an alternative point-coloring scheme. We shall see these rules are equally effective at preventing illegal overlaps in that case.

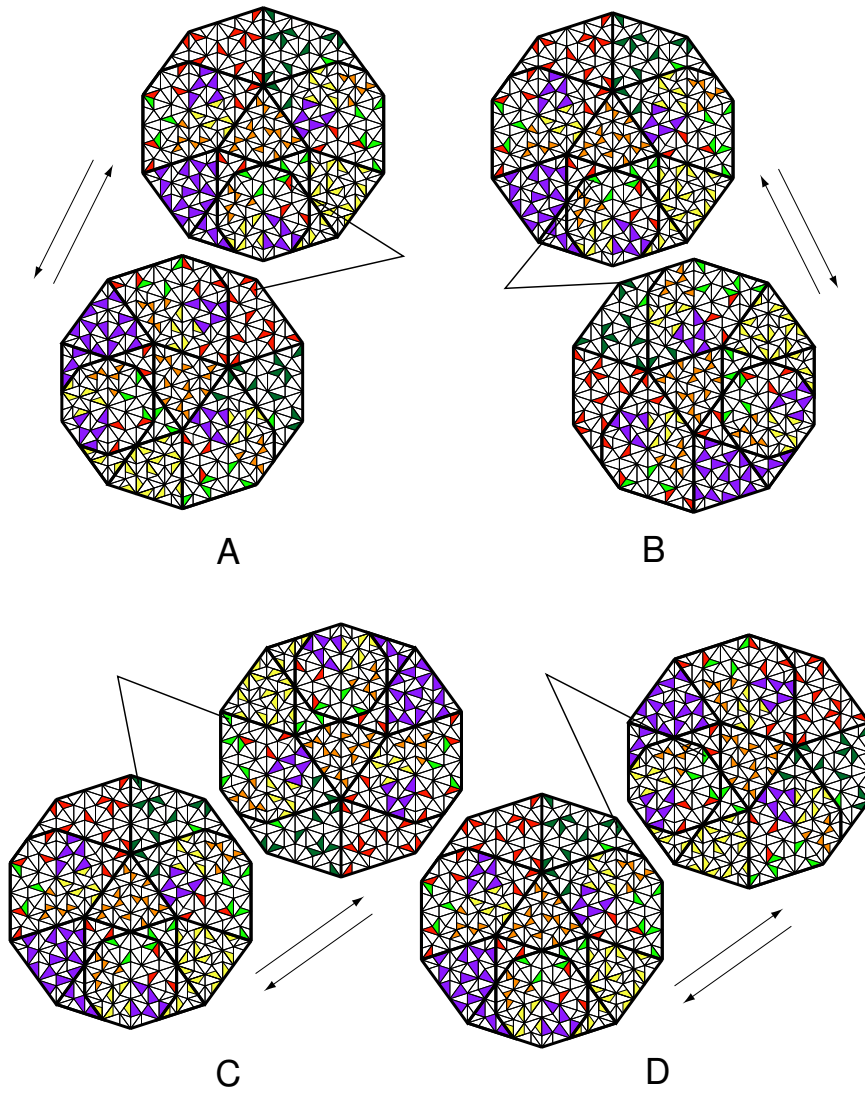


Figure 4.6: A, B, C and D are four illegal ways to tile two decagon sponges. Regions with conflicts are identified.

4.4 Conclusion

In this chapter, we present one possible construction of a decagonal sponge tile. Our analysis indicates that a minimum of five color sets are needed. The sponge we constructed consists of five color sets and the boundaries are colored black. The points in each color set spread throughout the tile but are dense only within a small region. We will seek an alternative method to define our color sets in the next chapter so that the sponge will be dense for each color set in every open ball.

Chapter 5

Second Construction of Color Sets

5.1 Introduction

Our purpose here is to construct sponges/Cantor sets that are measure positive in every open ball and no two sets intersect with each other. We will first consider 1-D “sponges” and try to mimic its construction for our 2-D sponges.

5.2 1-D Color Sets

In this section we will look at a simple 1-D case. Although we need a minimum of five color sets in 2-D, we will construct two 1-D sets first. Once we have the two sets, it is possible to construct more sets by recursive partitions. Thus our goal here is to find two disjoint sets of points such that given any interval $I \subseteq [0, 1]$, the measure of intersection between I and either of the sets is positive. Our construction is modified from [MRSZ97].

First we construct K , a Cantor set of measure $\frac{1}{2}$ in X , where $X = [0, 1]$. A traditional Cantor Set is of measure 0. We wish to fairly evenly divide the interval into two sets of positive measure. Define K by $K = X - \bigcup_{n=1}^{\infty} (B_n)$, where B_n is a countable union of open intervals defined as follows. Let B_1 be the central interval of length $\frac{1}{6}$. Given the construction of B_{n-1} , let B_n be the union of the central intervals of length $\frac{1}{2 \cdot 3^n}$ of the 2^{n-1} intervals remaining in $X - \bigcup_{i=1}^{n-1} (B_i)$. The first few steps are illustrated in Figure 5.1. We have:

$$\mu(K(X)) = 1 - \sum_{i=1}^{\infty} \frac{2^{i-1}}{2 \cdot 3^i} = 1 - \frac{1}{6} \cdot \frac{1}{1 - 2/3} = \frac{1}{2}$$

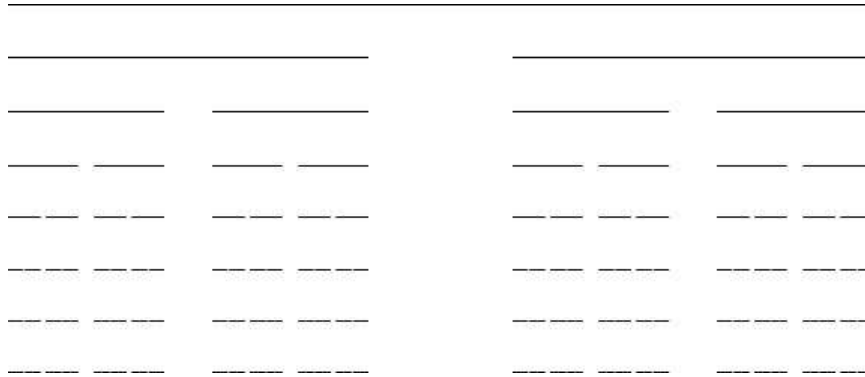


Figure 5.1: The first few steps in generating Cantor set.

Given an open interval $I \subset X$, define a modified Cantor set, denoted by $K(I)$, in the following way. Let $K' = K \setminus \{0, 1\}$. Scale the set K' by the factor $\mu(I)$ and place the scaled copy at the left end-point of I . Denote the new set by $K(I)$. This new set, a collection of intervals, scaled appropriately, has measure that is also scaled appropriately.

Now we proceed iteratively. Let $L_1 = K((0, \frac{1}{2}))$ and $R_1 = K((\frac{1}{2}, 1))$. Assume L_{n-1} and R_{n-1} have been defined. The complement in $(0, \frac{1}{2})$ or $(\frac{1}{2}, 1)$ of each of these sets consists of a countable disjoint collection of open intervals denoted A_i and B_i , respectively. Let $L_n = \bigcup_{i=1}^{\infty} K(A_i)$ and $R_n = \bigcup_{i=1}^{\infty} K(B_i)$. We note that L_1, L_2, \dots are each pairwise disjoint as are R_1, R_2, \dots

We finally define

$$S_1 = L_1 \cup R_2 \cup L_3 \cup R_4 \cup \dots \tag{5.1}$$

$$S_2 = R_1 \cup L_2 \cup R_3 \cup L_4 \cup \dots \tag{5.2}$$

It is easy to see that S_1 and S_2 are disjoint.

Lemma 3. *Given any interval $I \subseteq [0, 1]$, $\mu(I \cap S_1) > 0$ and $\mu(I \cap S_2) > 0$.*

*Proof*¹: We will first show that given any interval $I = (a, b) \subseteq [0, 1]$, if $\mu(I \cap S_1) > 0$ then $\mu(I \cap S_2) > 0$.

¹Modified from [MRSZ97]. Our interest, here, is to construct two symmetrically defined sets, which is slightly different than the referred work.

Let $x \in I \cap S_1$. Since every element of S_1 is in some $K(A)$ generated at stage n for some open interval A , $x \in I \cap K(A)$. Without loss of generality, assume $K(A) \subset L_n$. Moreover, $K(A)$ is perfect², which implies that for $\epsilon = \min\{x - a, b - x\} > 0$, there exists a $y \in K(A)$ such that $|x - y| < \epsilon$. Thus, $y \in I$. Since x and y are elements of the same $K(A)$ and $K(A)$ is totally disconnected, there must exist some open interval contained in $(\min\{x, y\}, \max\{x, y\})$ that is part of $K(A)^c \cap A$. In the construction of L_{n+1} , we know that at the $(n + 1)$ st stage, a set of positive measure $K(B)$ was constructed in that open interval, and $K(B) \subset L_{n+1} \subset S_2$. Hence,

$$\mu(S_2 \cap I) \geq \mu(K(B) \cap I) = \mu(K(B)) > 0.$$

By symmetry, we know that if $\mu(I \cap S_2) > 0$ then $\mu(I \cap S_1) > 0$. Also by symmetry, we know that any element $z \in S_1$ corresponds to an element $(1 - z) \in S_2$. It is easy to see that $\mu(\bigcup_{n=1}^{\infty} L_n \cup \bigcup_{n=1}^{\infty} R_n) = 1$. This implies that the points in S_1^c that do not correspond to elements in S_1 by the relation above amount to a set of measure zero, i.e., $\mu(S_1^c \setminus S_2) = 0$. Hence, $\mu(S_1^c) = \mu(S_2)$.

We know that $\mu(I \cap S_1) + \mu(I \cap S_1^c) = \mu(I) > 0$. Thus $\mu(I \cap S_1) + \mu(I \cap S_2) > 0$. Therefore, $\mu(I \cap S_1) > 0$ and $\mu(I \cap S_2) > 0$. \square

One useful condition for constructing Cantor sets with positive measure is that the percentage taken out from the remaining intervals has to decrease in each iteration. In our construction, in the n th stage, we take out intervals of $\frac{1}{2 \cdot 3^n}$ of the 2^{n-1} intervals remaining. At the $(n + 1)$ th stage, the length taken out in each interval becomes $\frac{1}{3}$ of that of the previous step and the number of intervals doubles. Thus such procedure guarantees that the percentage taken out decreases. Let us take a look at what happens if we take out a fixed percentage in each iteration.³

Lemma 4. *In the 1-D Cantor set construction, if a fixed positive percentage of the remaining intervals is taken out in each iteration, the construction will give us a Cantor Set with zero measure.*

Proof: Assume the percentage taken out is λ ($0 < \lambda \leq 1$). We will calculate the total length of the intervals taken out.

²A set S is perfect if it is closed and every point of S is an accumulation point of S .

³Interested readers can pursue further to see if it is possible to take out an increasing percentage of length each time.

At iteration i	Length taken out at iteration i
1	λ
2	$(1 - \lambda) \cdot \lambda$
3	$[1 - \lambda - (1 - \lambda) \cdot \lambda] \cdot \lambda = (1 - \lambda)^2 \cdot \lambda$
...	...
n	$(1 - \lambda)^{n-1} \cdot \lambda$
...	...

It is easy to see from the table above (or prove by induction) that at i th iteration, the length of the interval taken out is $(1 - \lambda)^{i-1} \cdot \lambda$. Thus the total length taken out is

$$\sum_{i=1}^{\infty} (1 - \lambda)^{i-1} \cdot \lambda = \frac{1}{1 - (1 - \lambda)} \cdot \lambda = 1$$

Therefore, all the points left amount to a set of measure zero. \square

5.3 2-D Color Set Construction

Based on the discussion about 1-D case, we are now ready to build our color sets in 2-D. Since we need 5 colors, we will construct 5 color sets, $\{S_1, S_2, S_3, S_4, S_5\}$ such that:

1. Each $S_i \subseteq T$ for some tile T in \mathfrak{R}^2 .
2. Distinct color sets S_i and S_j are disjoint.
3. Given any open ball B in τ , $\mu(B \cap S_i) > 0$.

Before we start our construction, we would like to identify an important feature of the Penrose tiling construction: Penrose tilings are prototile balanced. We will use the lemma below to prove it. We denote the results after inflating the Robinson's large and small A-tiles by a factor by $\tau\tau L_A$ and τS_A .

Lemma 5. *For integer $n > 0$, $\tau^n L_A = f_{2n+1} L_A + f_{2n} S_A$ and $\tau^n S_A = f_{2n} L_A + f_{2n-1} S_A$, where f_k is the k th term in the Fibonacci sequence*

$$1, 1, 2, 3, 5, 8, 13, 21, \dots$$

Proof: We will prove it by induction.

Base Case: The inflation rule (see Figure 1.7) tells us that each τL_A is composed of two L_A tiles and one S_A tile, and τS_A is composed of one L_A tile and one S_A tile. Hence we have counts of tiles defined recursively:

$$\begin{aligned}\tau L_A &= 2L_A + S_A \\ \tau S_A &= L_A + S_A\end{aligned}$$

Inductive Hypothesis: Assume that, for all positive values $k \leq n$:

$$\tau^k L_A = f_{2k+1}L_A + f_{2k}S_A \quad (5.3)$$

$$\tau^k S_A = f_{2k}L_A + f_{2k-1}S_A \quad (5.4)$$

Inductive Step: Consider $n + 1$:

$$\begin{aligned}\tau^{n+1} L_A &= \tau \cdot \tau^n L_A = \tau(f_{2n+1}L_A + f_{2n}S_A) \\ &= f_{2n+1}(2L_A + S_A) + f_{2n}(L_A + S_A) \\ &= (f_{2n+1} + (f_{2n+1} + f_{2n}))L_A + (f_{2n+1} + f_{2n})S_A \\ &= (f_{2n+1} + f_{2n+2})L_A + f_{2n+2}S_A \\ &= f_{2n+3}L_A + f_{2n+2}S_A \\ &= f_{2(n+1)+1}L_A + f_{2(n+1)}S_A\end{aligned}$$

$$\begin{aligned}\tau^{n+1} S_A &= \tau \cdot \tau^n S_A = \tau(f_{2n}L_A + f_{2n-1}S_A) \\ &= f_{2n}(2L_A + S_A) + f_{2n-1}(L_A + S_A) \\ &= (f_{2n} + (f_{2n} + f_{2n-1}))L_A + (f_{2n} + f_{2n-1})S_A \\ &= (f_{2n} + f_{2n+1})L_A + f_{2n+1}S_A \\ &= f_{2(n+1)}L_A + f_{2(n+1)-1}S_A\end{aligned}$$

Therefore, the lemma holds. \square

From the lemma above, we have the following corollary:

Corollary 1. *Let S be any patch of $\tau^n L_A$ and $\tau^n S_A$ from a $\tau^n A$ tiling. Let $r(S)$ be the ratio of number of large A -tiles L_A to the number of small A -tiles S_A in such a region. We have:*

$$\frac{f_{2n}}{f_{2n-1}} \leq r(S) \leq \frac{f_{2n+1}}{f_{2n}} \quad (5.5)$$

Proof: If A consists of L_A tiles only, according to our lemma, we have $r(S) = \frac{f_{2n+1}}{f_{2n}}$. Similarly, if A consists of S_A tiles only, we have $r(S) = \frac{f_{2n}}{f_{2n-1}}$. Since A here is formed by a mix of L_A and S_A tiles and we know that $\frac{f_{2n}}{f_{2n-1}} < \frac{f_{2n+1}}{f_{2n}}$,⁴ hence we have $\frac{f_{2n}}{f_{2n-1}} \leq r(S) \leq \frac{f_{2n+1}}{f_{2n}}$. \square

We are now able to state and prove the following theorem:

Theorem 3. *Every tiling by Penrose kites and darts is prototile balanced: the ratio of the average number of kites and the average number of darts per unit area of the plane is the golden ratio.*

Proof: From equation 5.5 and the fact that $f_{n+1}/f_n \rightarrow \tau$ as $n \rightarrow \infty$, we have $\lim_{n \rightarrow \infty} r(S) = \tau$. \square

As every Penrose tiling can also be tiled by Robinson's large A and small A tiles, we will consider Robinson's A tile first. Analogous to our 1-D approach, we need to accomplish the following steps:

1. Define an operation K for an area.
2. Perform K operations iteratively on pieces taken out.
3. Define 5 disjoint sets.
4. Prove they are measure positive in every open ball.

In the end, we will note that every point is a member of some color set.

Robinson's inflation rules provide a great start for constructing our K operation. A natural way to define our K operation would be to take out all small A tiles in each inflation of large A tiles. However, as in each inflation, the percentage area of small A tiles is constant, similar to the 1-D Cantor set discussed in Lemma 4, this approach will leave us with a set of measure zero. Analogous to the modified Cantor Set approach, we need to take out less area in each iteration. The difficulty here is that it is not obvious which subtiles to take out, whereas in 1-D case we can exactly specify the length of the central interval to be taken out.

In order to specify the pieces to be taken out in each stage, we will need to define an *address* for each Robinson's tile in the decomposition process.

⁴We shall note that in general, $\frac{f_n}{f_{n-1}}$ is not necessarily less than $\frac{f_{n+1}}{f_n}$. (Consider $n = 3$.) However, in all cases, $|\frac{f_n}{f_{n-1}} - \tau| > |\frac{f_{n+1}}{f_n} - \tau|$.

First we denote Robinson's left handed large A tile, right handed large A tile, left handed small A tile and right handed small A tile to be L , L' , S and S' respectively. After decomposing Robinson's tile n times, we will obtain many small L_A and S_A tiles. The address of any of these tiles can be written as $A_0A_1A_2 \cdots A_n$, where $A_i = \mathcal{T} \in \{L, L', S, S'\}$, if the tile is in \mathcal{T} at i th stage. Consider the example as shown in Figure 5.2. The tile pointed at is generated by decomposing Robinson's left handed large A tile three times. The locations of this tile in each decomposition (including the original location) are left handed large A tile, right handed large A tile, left handed large A tile and left handed small A tile. Therefore, the address of the tile is $LL'L'S'$. It is easy to see that there is a bijection between the tile and its address.

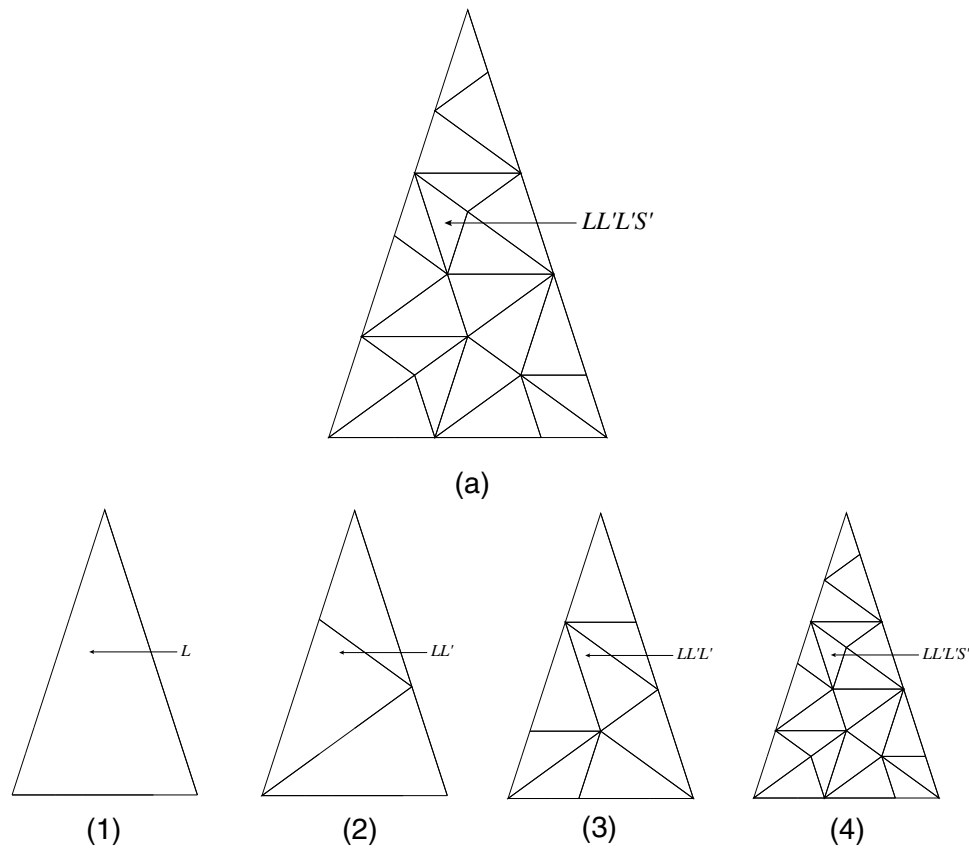


Figure 5.2: The address of the tile pointed at in (a) is $LL'L'S'$. Figure (1)-(4) shows each step in determining the address of the tile.

Once we know the address for each tile in the decomposition, we will be able to remove a goal percentage of the remaining area at each iteration. However, as we are removing tiles, it will not be possible to remove the percentage exactly. Instead, we seek to remove the percentage with accuracy measured by an error term ϵ , which we may make arbitrarily small.

We first construct K , a 2-D *Cantor Set* of positive measure in T , where T is either a Robinson's large A tile (L_A) or small A tile (S_A), by the following steps:

1. Decompose the tile or the remaining tiles ($c + i$) levels for an appropriate c (determined by desired ϵ). This c helps determine the percentage removed within bounds.
2. Imagine tiles have addresses determined by size of tile at each expansion, eg. $LSLLSLS \cdots SS$ remove all open tiles that end in i number of S (include S') terms. Note we will keep the boundary of the tile intact. This effectively makes our removal more selective. The percentage will significantly decrease in each stage, but can be made within ϵ of $(\frac{1}{\tau^2+1})(\frac{1}{\tau^2})^{i-1}$ for stage $i \geq 1$.
3. Repeat with $i \leftarrow i + 1$.

Notice that $T - K(T)$ is a countable collection of open small A tiles. Now we proceed iteratively. Let $K_0(T) = T$, $K_1(T) = K(T)$. We define:

$$K_i(T) = K(K_{i-2}(T) - K_{i-1}(T))$$

Finally we define our five color sets to be:

$$S_i(T) = \bigcup_{k=0}^{\infty} K_{5k+i}(T)$$

where $i = 1, 2, 3, 4, 5$.

5.3.1 Analysis

We would like to know the measure for each color set. To compute that, we need to know $\mu(K(T))$ first. We know from equation 5.3 that we will have f_{2n+1} large A-tiles and f_{2n} small A-tiles. Because each large A-tile is τ larger than small A-tile, the total area of large A-tiles is $\frac{\tau \cdot f_{2n+1}}{f_{2n}}$ larger than that of small A-tiles. When $n \rightarrow \infty$, the area of large A-tiles is τ^2 larger than small A-tiles.

We let the initial area of Robinson's tile be $A(T)$. T is either a Robinson's large A tile or a Robinson's small A tile. We have:

After i th Step	Area Removed (R_i) (L tile)	Area Removed (R_i) (S tile)
1	$\frac{A(L) \cdot f_{2c}}{\tau f_{2c+1} + f_{2c}}$	$\frac{A(S) \cdot f_{2c-1}}{\tau f_{2c} + f_{2c-1}}$
2	$\frac{(A(L) - R_1) \cdot f_{2(2c-1)} \cdot \frac{1}{\tau^2}}{\tau f_{2(2c-1)+1} + f_{2(2c-1)}}$	$\frac{(A(S) - R_1) \cdot f_{2(2c-1)-1} \cdot \frac{1}{\tau^2}}{\tau f_{2(2c-1)} + f_{2(2c-1)-1}}$
3	$\frac{(A(L) - R_1 - R_2) \cdot f_{2(3c-2)} \cdot \left(\frac{1}{\tau^2}\right)^2}{\tau f_{2(3c-2)+1} + f_{2(3c-2)}}$	$\frac{(A(S) - R_1 - R_2) \cdot f_{2(3c-2)-1} \cdot \left(\frac{1}{\tau^2}\right)^2}{\tau f_{2(3c-2)} + f_{2(3c-2)-1}}$
.
k	$\frac{(A(L) - \sum_{i=1}^{k-1} R_i) \cdot f_{2(kc-(k-1))} \cdot \left(\frac{1}{\tau^2}\right)^{k-1}}{\tau f_{2(kc-(k-1))+1} + f_{2(kc-(k-1))}}$	$\frac{(A(S) - \sum_{i=1}^{k-1} R_i) \cdot f_{2(kc-(k-1))-1} \cdot \left(\frac{1}{\tau^2}\right)^{k-1}}{\tau f_{2(kc-(k-1))} + f_{2(kc-(k-1))-1}}$
.

Thus the remaining area, i.e., $\mu(K(T))$, is $A(T) - \sum_{i=1}^{\infty} R_i$. This sum is not easy to compute directly. However, we know as $n \rightarrow \infty$, $\frac{f_{2n+1}}{f_{2n}} \rightarrow \tau$. Hence, $\frac{f_{2n}}{\tau \cdot f_{2n+1} + f_{2n}} \rightarrow \frac{1}{\tau^2 + 1}$. We can therefore approximate R_i . Let $A(T) = 1$. We have:

After i th Step	Area Removed	Area Remaining
1	0.276393	0.723607
2	0.352786	0.647214
3	0.378885	0.621115
4	0.388452	0.611548
5	0.392050	0.607950
6	0.393417	0.606583
7	0.393937	0.606063
8	0.394136	0.605864
9	0.394212	0.605788
10	0.394241	0.605759
20	0.394259	0.605741
50	0.394259	0.605741
100	0.394259	0.605741

Thus we have an area with measure 0.605741 left. That is, around 60 percentage area left for both large and small tiles.

Lemma 6. *The larger the c is, the smaller error our approximation will have.*

Proof: Without loss of generality, we will use Robinson's large A tile to prove this lemma. Assume that $A(L) = 1$. Let $e = \left| R_1 - \frac{1}{\tau^2 + 1} \right|$. Since the term $A(L) - \sum_{i=1}^{k-1} R_i < 1$ and $\left| \frac{f_{2(kc-(k-1))}}{\tau \cdot f_{2(kc-(k-1))+1} + f_{2(kc-(k-1))}} - \frac{1}{\tau^2 + 1} \right|$ is smaller as c increases, the total

error for $1 - \sum_{i=1}^{\infty} R_i$ is bounded by $e + e^{\frac{1}{\tau^2}} + e(\frac{1}{\tau^2})^2 + \dots + e(\frac{1}{\tau^2})^k + \dots = e \frac{1}{1 - \frac{1}{\tau^2}} = \frac{e\tau^2}{\tau^2 - 1} = \frac{e\tau^2}{\tau} = e\tau$. Thus the total error is:

$$\left| \frac{f_{2c}}{\tau \cdot f_{2c+1} + f_{2c}} - \frac{1}{\tau^2 + 1} \right| \cdot \tau$$

We know that as c increases, f_{2c+1}/f_{2c} monotonically decreases towards τ . Thus, $\frac{f_{2c}}{\tau \cdot f_{2c+1} + f_{2c}} = \frac{1}{\tau \cdot f_{2c+1}/f_{2c} + 1}$ will become closer to $\frac{1}{\tau^2 + 1}$ from below. Therefore, the total error decreases as c increases. \square

We now would like to investigate the relationship between c and a given ϵ . Now, given a desired value of ϵ , what is the minimum value c necessary? (We know c will be bounded below because of the lemma we proved above.) Hence, we have

$$\left| \frac{f_{2c}}{\tau \cdot f_{2c+1} + f_{2c}} - \frac{1}{\tau^2 + 1} \right| \cdot \tau < \epsilon$$

We also know the following for the Fibonacci sequence :

$$f_{n+1} = \tau f_n + \hat{\tau}^n$$

where $\hat{\tau} = \frac{1 - \sqrt{5}}{2}$.

Hence, we have:

$$\frac{\hat{\tau}^{2c}}{f_{2c}} < \frac{\epsilon(1 + \tau^2)^2}{-\epsilon\tau + \tau^2 - \epsilon\tau^3}$$

We also know that

$$f_n = \frac{1}{\sqrt{5}}(\tau^n - \hat{\tau}^n)$$

Thus we have:

$$\left(\frac{\tau}{\hat{\tau}}\right)^{2c} > \sqrt{5} \cdot \frac{-\epsilon\tau + \tau^2 - \epsilon\tau^3}{\epsilon(1 + \tau^2)^2} + 1$$

That is:

$$c > \frac{1}{2} \cdot \log_{(-\tau/\hat{\tau})} \left(\sqrt{5} \cdot \frac{-\epsilon\tau + \tau^2 - \epsilon\tau^3}{\epsilon(1 + \tau^2)^2} + 1 \right) \quad (5.6)$$

The below are some results based on 5.6:

ϵ	Minimum c Required
10^{-1}	1
10^{-2}	2
10^{-3}	4
10^{-10}	12
10^{-20}	24
10^{-30}	36
10^{-100}	120

Our empirical results match with the theoretical work well. With our approximation scheme, the area left is

$$0.605, 741, 297, 360, 287, 501, 307, 977, 266, 5.$$

When $c = 1$, the exact area remaining is 0.65690, which is within 0.1 of the result from approximation. When $c = 2$, the exact area left is 0.61090, which is within 0.01 the result from approximation. When $c = 12$, the exact area left is

$$0.605, 741, 297, 381, 810, 618, 528, 068, 403, 5.$$

the two numbers differ at 11th decimal position, i.e., the difference is within 10^{-10} . These results support our predictions in the table above. Indeed, the greater the value of c is, the smaller the error will be.

Now we are ready to compute the measure for each color set, i.e., the percentage of area of each color set in the tile T . Since each K operation will leave 60.57% of the area which it is applied on, it is easy to see the following:

$$\begin{aligned} \mu(K_1(T)) &= 0.6057 \\ \mu(K_2(T)) &= 0.6057 \cdot (1 - \mu(K_1(T))) \\ \mu(K_3(T)) &= 0.6057 \cdot (1 - \mu(K_1(T)) - \mu(K_2(T))) \\ &\dots \\ \mu(K_i(T)) &= 0.6057 \cdot \left(1 - \sum_{j=1}^{i-1} \mu(K_j(T))\right) \\ &\dots \end{aligned}$$

Recall our definition for each color set:

$$S_i(T) = \bigcup_{k=0}^{\infty} K_{5k+i}(T)$$

where $i = 1, 2, 3, 4, 5$.

Since each $K_i(T)$ are distinct, i.e., all sets are pairwise disjoint, we have:

$$\mu(S_i(T)) = \sum_{k=0}^{\infty} \mu(K_{5k+i}(T))$$

Thus we can compute the measure of the each color set as below:

$$\begin{aligned} \mu(S_1(T)) &= 0.61152 \\ \mu(S_2(T)) &= 0.24112 \\ \mu(S_3(T)) &= 0.09507 \\ \mu(S_4(T)) &= 0.03748 \\ \mu(S_5(T)) &= 0.01478 \end{aligned}$$

Notice that $\sum_{i=1}^5 \mu(S_i(T)) = 1$ since all $K_i(T)$ sum to 1.

We are now going to prove that each of these color sets is measure positive everywhere in the tile.

Lemma 7. *Given any open ball B in T , $\mu(B \cap S_i) > 0$ for $i = 1, 2, 3, 4, 5$.*

Proof: It is easy to see that there exists a Robinson's small tile, t , such that t is entirely within B . At some later stage in construction of $K_n(T)$, a positive percentage of t will be removed. We know a set $K(t)$, $K(t) \subset K_{n+1}(T)$, will be constructed in t . Therefore, $\mu(K_{n+1}(T)) \geq \mu(K(t)) > 0$. That is, since $K_{n+1} \subset S_i$ for some i , $\mu(B \cap S_i) > \mu(B \cap K_{n+1}) \geq \mu(K(t)) > 0$. Since n can be any integer as long as it is sufficiently large, we can similarly show $\mu(B \cap S_i) > 0$ for $i = 2, 3, 4, 5$. \square

5.4 Our Decagonal Sponge Tile

As the decagonal tile (see 4.2) can be tiled by Robinson's large and small A tiles, we will construct our decagonal sponge tile according to our previous coloring scheme. We will first associate colors with our 5 sets:

$$\begin{aligned} S_T(\text{Red}) &= S_1(T) \\ S_T(\text{Green}) &= S_2(T) \\ S_T(\text{Orange}) &= S_3(T) \\ S_T(\text{Yellow}) &= S_4(T) \\ S_T(\text{Purple}) &= S_5(T) \end{aligned}$$

Then for any subtile T with color c in the decagon (T can be either a Robinson's large A tile or Robinson's small A tile), we will fill the region with $S_T(c)$. Finally, we will color all the internal boundaries to be gray and external boundaries to be black. Now we have constructed our sponge tile! Figure 5.3 shows a rough appearance of our sponge tile.

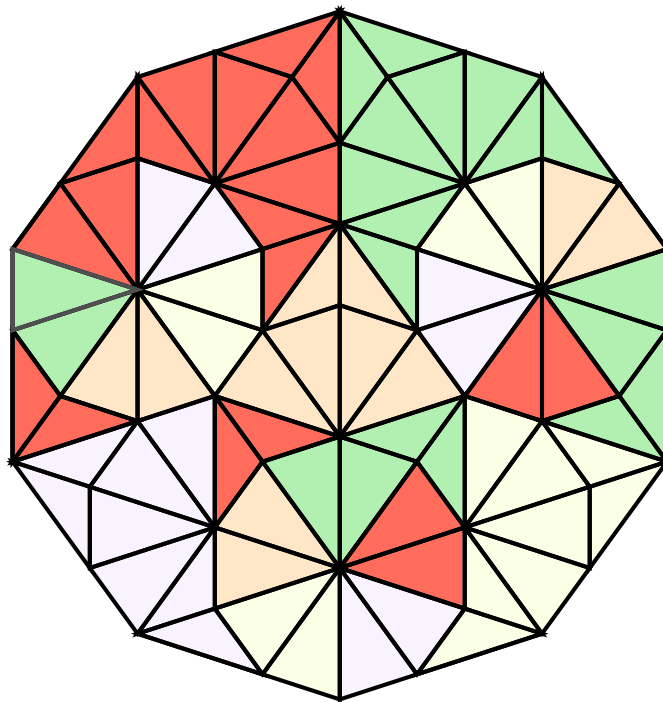


Figure 5.3: Our decagonal sponge tile. As color sets have different measures, their densities differ in the tile.

5.4.1 Matching Rules of the Sponge Tile

The matching rules for our sponge tile are the same as the matching rules we developed in our first construction. That is, external edges of some tile must be covered by internal edges of other tiles,⁵ and no region, as defined in Figure 4.1, can be tiled by more than one sponge with a given color. Our sponges also prevent these illegal 'tilings' shown in Figure 4.6 except that the regions are now filled with Cantor-like

⁵Alternatively, we can state this matching rule as all black points must be covered by gray points

sponges. Just like in a normal Penrose tiling, boundaries are allowed to overlap with each other in our sponge tiling. Since the measure for any line segment in 2-D is zero, such overlapping will not change the measure for our decagon sponge.

5.4.2 Aperiodicity of the Sponge Tile

First we need to note that Gummelt's decagon *covering* has been converted to decagon *tiling* by our construction. In each of the overlapping region in Gummelt's covering is now replaced by several measure positive sets of points, each with different colors from others. As our construction ensures that any two sets with different colors must be disjoint with each other, no points will collide at any position. The aperiodicity of the sponge tile is inherited from that of the Gummelt's decagon covering. Since Gummelt's has shown that her decagon covering is aperiodic and there is a bijection between our decagonal sponge tiling and her decagon covering, the sponge tiling must be aperiodic.

5.5 A Bin-Packing Approach

While in our construction the color sets all have positive measures, their measures have remarkable difference. Ideally, we would like each color set to have approximately the same measure. If we recall our 1-D construction, in which we were able to evenly divide a unit interval into two color sets by first dividing it into two segments, we might ask ourselves whether we can do something similar in our 2-D construction. The difficulty of the 2-D case lies in the irregular shapes of the tiles. It is unlikely that the tiles we could still follow Robinson's inflation rules after we divide them into even pieces. Here, we present an alternative approach — a bin-packing algorithm — to achieve this goal.

We will start with five bins, b_1, b_2, b_3, b_4 and b_5 , each represents one color set. Our algorithm will assign points generated from each K operation to the five bins such that each bin will have measure 0.2 at the end. As $\mu(K_1) = 0.6057 > 0.2$, we will need to modify K operation slightly so that we will be able to fit every point set into one of the bins. Rather than starting with taking away areas according to the number of S 's in the tile address, we will use the number of L 's in the tile address instead. We can similarly compute each $\mu(K_i)$. We have $\mu(K_1) = 0.0157$, $\mu(K_2) = 0.0154$, $\mu(K_3) = 0.0152, \dots$

Now we are ready to perform our bin-packing algorithm to assign each point set into an appropriate bin. Figure 5.5 illustrates the basic idea of this algorithm.

```

i ← 1;
while(true) {
  j ← 1;
  while( $\mu(b_j) + \mu(K_i) \geq 0.2$ )
    j ← j + 1;
  add  $K_i$  to  $b_j$ ;
  i ← i + 1
}

```

Figure 5.4: A bin-packing algorithm for assigning color sets. This algorithm evenly distributes points sets into 5 bins.

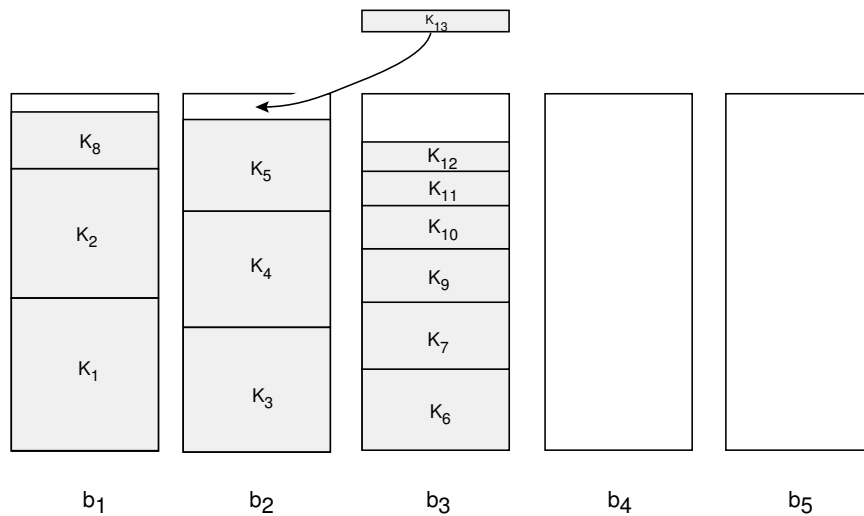


Figure 5.5: An illustration of our bin-packing algorithm. Boxes are not drawn to scale. Here we are trying to find an available slot for K_{13} by checking each bin in sequence. K_{13} will be added to b_2 in this case.

In order for the algorithm to run correctly, we need to make sure that the inner while loop will always exit for $j \leq 5$. Recall that $\mu(K_i(T)) = \mu(K_1) \cdot (1 - \sum_{j=1}^{i-1} \mu(K_j(T)))$, where $\mu(K_1)$ in this case is 0.0157. Essentially, in the i th step, we are trying to find a slot in one of the bins to accommodate 1.57% of the total unfilled area. Since we have 5 bins, there is at least one bin whose unfilled area is no less than 20% of the total unfilled area. Therefore, we are always able to find such slot. This frees us from the need to check the condition $j \leq 5$ in the inner while loop.

At the end, we assign each bin to a distinct color and the tile can be constructed in exactly the same way as shown in Figure 5.3 except that each color now has the same density. We should also notice that the condition $\mu(b_j) + \mu(K_i) \geq 0.2$ will avoid each bin being completely filled during our iterations. That is, each bin will be filled by an infinite number of point sets. It is therefore easy to give a similar proof as in Lemma 7 that the point sets in each bin have positive measure in any open ball.

Empirical results indicate that after assigning the first 700 point sets from K operation, the measure of each bin, i.e., the measure of each color set, will be within 10^{-5} from 0.2.

5.6 Conclusion

In this chapter, we present an alternative construction for our decagonal sponge. The construction is Cantor-like and based on recursive refilling. The sponge has five color sets, each with positive measures. We have also proved that the sponge constructed is measure positive in every open ball and a tiling formed by the sponge following overlapping rules must be aperiodic.

Chapter 6

Conclusions and Future Work

6.1 Conclusions

Although our work did not find a universal tile, we have shown that it is possible to construct a single sponge tile that tiles the 2-D space aperiodically. Many previous attempts involve breaking rules. The fractal tile approach extends the notion of edges to include those of zero length; Gummelt's decagon covering allows tiles to overlap in a controlled fashion. Our sponge approach is similar in this respect. Essentially, we extend the notion of tiles to include those with non-solid interiors. All these attempts demonstrate completely different ways to search for the universal tile. They all help us gain a better understanding of the structure of aperiodic tiles. As there is still no known mechanism of generating a universal tile, it is crucial for us to have various possible approaches.

We also introduced *measure* into our construction of the sponges. Although our sponge tile does not have solid interior, it has positive measure in any open ball. That is, the points are dense enough to constitute an area everywhere.

An aperiodic tiling with overlapping areas is useful because it exhibits a structure similar to quasi-crystals. For example, one way to model the structure of $\text{Al}_{72}\text{Ni}_{20}\text{Co}_8$, one of the best-characterized quasicrystalline materials and an excellent candidate for comparing structural models of quasicrystals, is to use a decagon. A micrograph of its structure is found in Figure 6.1. If we take a close look at a sample formed by $\text{Al}_{72}\text{Ni}_{20}\text{Co}_8$ (see Figure 6.2), the interactions between atoms can be modelled by Gummelt's decagonal covering and our decagonal tiling. [AST⁺00]

Recent research has indicated that the interaction between two atoms should be best interpreted as sharing instead of overlapping. Our sponge approach incorporates

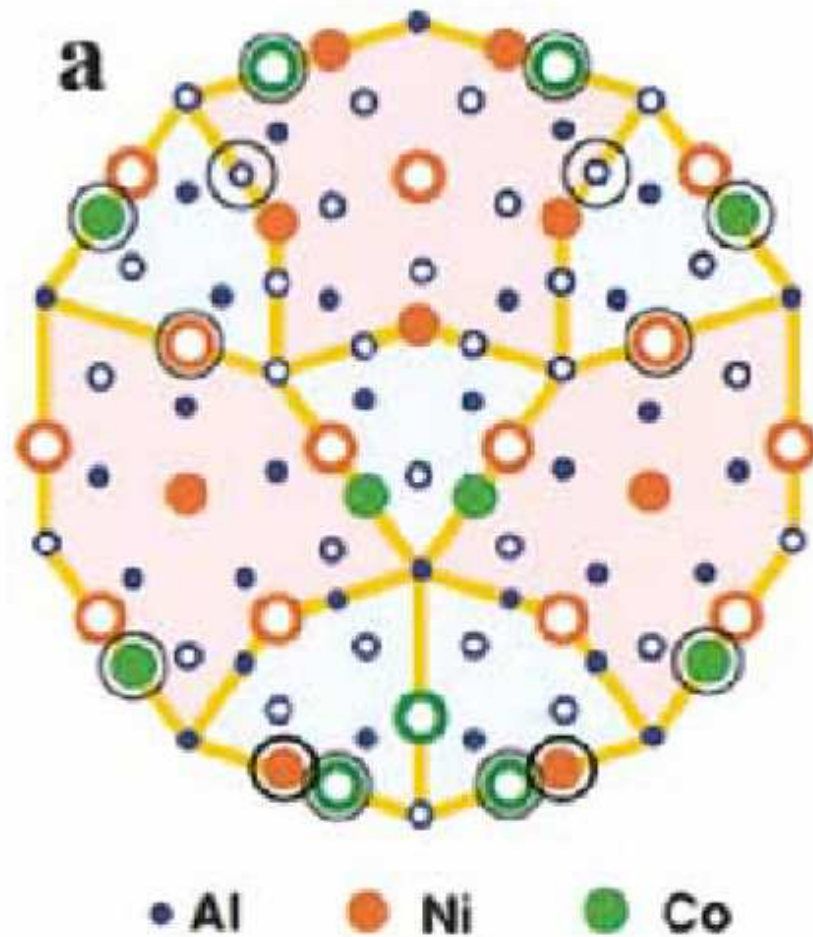


Figure 6.1: Atomic decoration of the decagonal (2nm) quasi-unit cell for $\text{Al}_{72}\text{Ni}_{20}\text{Co}_8$. Every local neighborhood of $\text{Al}_{72}\text{Ni}_{20}\text{Co}_8$ is similar to a decagon. [AST⁺00]

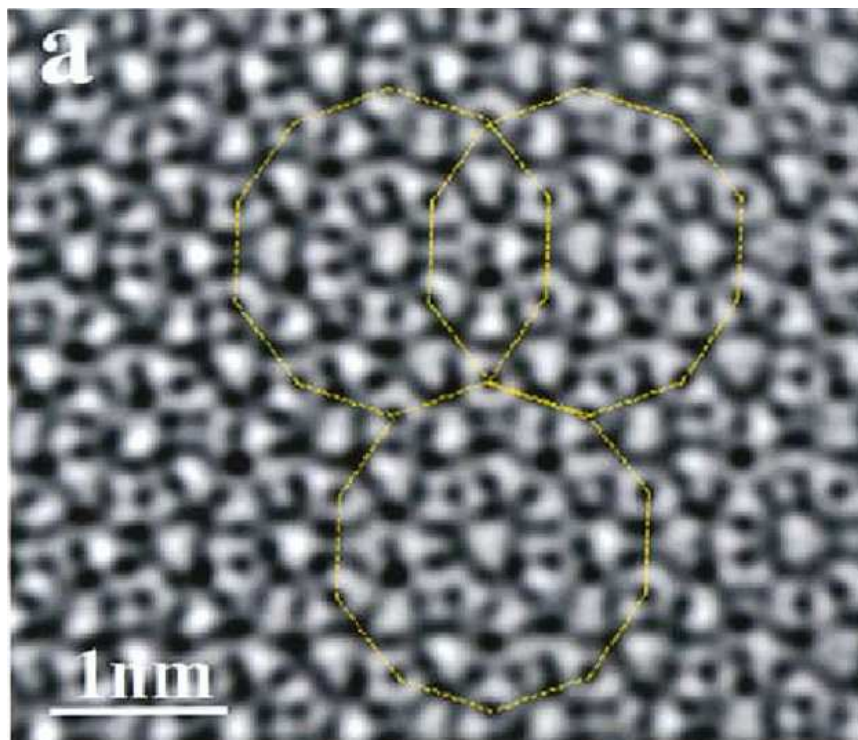


Figure 6.2: Image of the high quality sample of $\text{Al}_{72}\text{Ni}_{20}\text{Co}_8$.

notions of interleaving, density and diffusion. Therefore, the sponge might be a better model than the decagon covering.

6.2 Future Work

We believe that the notion of “mixing” we developed in our sponge construction will also work for higher dimensions. In 3-D, one possible approach is to work on icosahedral quasicrystal packings, which are formed by rhombohedrons, dodecahedrons, icosahedrons and triacontahedrons [SS86]. We believe it is possible to construct a 3-D aperiodic sponge by taking points from each configuration.

It is also possible to consider cartwheels with orders greater than one (recall the decagon is a first-order cartwheel). It is likely, as the order increases, that the percentage of overlapping regions will become smaller. We also believe that there is a lower bound for this percentage. Overlapping rules should also be redefined to ensure the aperiodicity of the coverings.

Appendix A

Cantor Set

In our constructions, we often use the ideas from the standard Cantor set construction. For the sake of completeness, we present its construction here.

The standard Cantor set is also called the *Cantor Middle Third Set*. It is constructed by the following algorithm:

```

$$\begin{aligned} S_0 &\leftarrow [0, 1] \\ i &\leftarrow 1 \\ \text{while}(\text{true}) \{ \\ & S_i \leftarrow S_{i-1} \setminus \{\text{middle thirds of open subintervals of } S_{i-1}\} \\ & i \leftarrow i + 1 \\ \} \\ \text{Cantor Set} &= \bigcap_{i=0}^{\infty} S_i \end{aligned}$$

```

Figure A.1: An algorithm for generating the standard cantor set. The standard cantor set will have measure 0 at the end.

At the i -th iteration ($i > 0$), we remove 2^{i-1} subintervals from each previous set, each having length $\frac{1}{3^i}$. Therefore, the total length we remove is:

$$\sum_{i=1}^{\infty} \frac{2^{i-1}}{3^i} = \frac{1}{3} \cdot \sum_{i=0}^{\infty} \left(\frac{2}{3}\right)^i = \frac{1}{3} \cdot \frac{1}{1 - 2/3} = 1$$

As a set of total length 1 is removed from interval $[0, 1]$, the length of the Cantor set is 0. That is, the measure of the standard Cantor set is 0.

Appendix B

Methods for Finding Fixed Points

In Chapter 4, we discussed a method of assigning a unique color to any point in 2-D space. We also pointed out that most points have indecisive colors in their color sequences. Here we consider the problem of finding fixed points, i.e., the points which ultimately preserve the original color during infinite decomposition. We use one of the Robinson tiles to illustrate our methods.

B.1 Method 1: Play with Geometry

As shown in Figure B.1, we let P be a fixed point in the right hand kite. Note P must be in the right hand of the kites. Because of the composition, we have $OP = \tau \cdot PM$ and $\angle POM = \angle PMN$.

We have, in $\triangle OPM$:

$$OP : PM = \sin\left(\frac{2\pi}{5} - \theta\right) : \sin \theta \quad \left(0 < \theta < \frac{2\pi}{5}\right)$$

Hence, we have $\theta = 0.45458$ (26.2677°)

Point P is simply the intersection between the following two lines:

$$\begin{aligned} y &= x \cdot \tan \theta \\ y &= (x - \tau) \cdot \tan\left(\frac{3\pi}{5} + \theta\right) \end{aligned}$$

Solving the two equations, we have $P = (1.09247, 0.539168)$

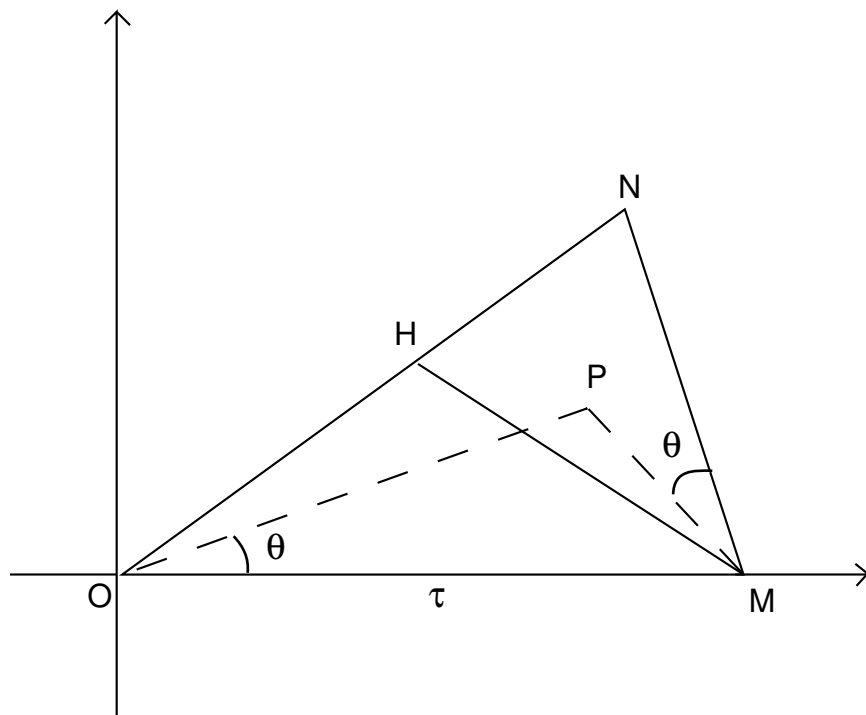


Figure B.1: Right handed Robinson's A tile.

B.2 Method 2: Use Mapping Function

Let f denote the mapping transformation from $\triangle OPM$ to $\triangle HMN$. f is given by $f_3(z) = \frac{z}{\tau} \cdot \omega_3 + \tau$, where $\omega_k = \cos(\frac{k\pi}{5}) + i \sin(\frac{k\pi}{5})$, z is any point in $\triangle OPM$ in complex coordinates. Point P has the property that

$$z_p = f(z_p) \tag{B.1}$$

Hence, $z_p = 1.09247 + 0.539168i$, i.e. $P = (1.09247, 0.539168)$

Equation A.1 guarantees that under any further inflations, P will preserve its color.

B.3 Summary

The second approach is more convenient and we can use it to find other fixed points under the other two transformation functions:

$$f_1(z) = \frac{z}{\tau} \cdot \omega_6 + \frac{\tau}{2} + i \sin \frac{\pi}{5} \tag{B.2}$$

$$f_2(z) = \frac{z}{\tau} \cdot \omega_3 + \tau \tag{B.3}$$

Notice that during inflation, f_2 always transforms A tile to left-hand of a kite, an A tile; f_3 always transforms A tile to the right-hand side of a kite, also an A tile; f_1 always transform a B tile to another B tile.

But are these the only three fixed points? Of course not. As we define “fixed” points as ones ultimately preserve a single color, we also allow a point to undergo a finite number of transforms before it starts to keep its color forever. Thus, there are many of these fixed points.

Appendix C

Postscript for Generating Fractal Tiles

Postscript is a stack-based interpreted language with powerful graphics capabilities. We found it very helpful in visualizing structures of the tilings. Here we present the code for generating fractal tiles discussed in Chapter 2. You may refer to Postscript references published by Adobe Systems to understand the code.

```
%!PS-Adobe-1.0
%% BoundingBox:
% $Id: factaltile.ps,v 0.1 2002/01/20 Feng Zhu$
% $Log: factaltile.ps,v$

% Setting both to true will print both tiles on the same page
/printDart true def
/printKite true def

% Level of decomposition
/depth 10 def

% golden mean
/golden 2 36 cos mul def

% Decompose a kite and perform transformation on it recursively
/ExpandKite {
    dup 0 gt {
```

```

1 sub

gsave
0 1 golden div 72 mul translate
108 rotate
1 golden div dup scale
dup ExpandKite
grestore

gsave
0 1 golden div 72 mul translate
-108 rotate
1 golden div dup scale
dup ExpandKite
grestore

gsave
1 golden div 72 sin mul 72 mul golden 1 golden div
  72 cos mul sub 72 mul translate
144 rotate
1 golden div dup scale
ExpandDart
grestore
}
% base case
{
  pop

  newpath
  0 0 moveto
  0 1 golden div 72 mul lineto
  1 golden div 36 sin mul -72 mul 1 golden div
    36 cos mul 1 golden div add 72 mul lineto
  18 cos -72 mul 18 sin 72 mul lineto
  0 0 lineto
  stroke

  newpath

```

```

    0 0 moveto
    0 1 golden div 72 mul lineto
    1 golden div 36 sin mul 72 mul 1 golden div
      36 cos mul 1 golden div add 72 mul lineto
    18 cos 72 mul 18 sin 72 mul lineto
    0 0 lineto
  stroke

  newpath
  0 golden 72 mul moveto
  0 1 golden div 72 mul lineto
  1 golden div 36 sin mul 72 mul 1 golden div
    36 cos mul 1 golden div add 72 mul lineto
  0 golden 72 mul lineto
  golden 1 golden div sub 72 mul 72 sin mul golden 72 mul
    golden 1 golden div sub 72 mul 72 cos mul sub lineto
  1 golden div 36 sin mul 72 mul 1 golden div
    36 cos mul 1 golden div add 72 mul lineto
  stroke
}
  ifelse
} def

% Decompose a Dart and perform transformation on it recursively
/ExpandDart {
  dup 0 gt {
    1 sub

    gsave
    1 golden div 72 sin mul 72 mul golden 1 golden div
      72 cos mul sub 72 mul translate
    144 rotate
    1 golden div dup scale
    dup ExpandDart
    grestore

    gsave
    0 1 golden div 72 mul translate

```

```

        -108 rotate
        1 golden div dup scale
        ExpandKite
        grestore
    }
% base case
{
    pop

    newpath
    0 0 moveto
    0 1 golden div 72 mul lineto
    1 golden div 36 sin mul 72 mul 1 golden div
      36 cos mul 1 golden div add 72 mul lineto
    18 cos 72 mul 18 sin 72 mul lineto
    0 0 lineto
    stroke

    newpath
    0 golden 72 mul moveto
    0 1 golden div 72 mul lineto
    1 golden div 36 sin mul 72 mul 1 golden div
      36 cos mul 1 golden div add 72 mul lineto
    0 golden 72 mul lineto
    golden 1 golden div sub 72 mul 72 sin mul golden 72 mul
      golden 1 golden div sub 72 mul 72 cos mul sub lineto
    1 golden div 36 sin mul 72 mul 1 golden div
      36 cos mul 1 golden div add 72 mul lineto
    stroke
}
ifelse
} def

% main procedure
printDart printKite and {
    gsave
    7 golden sub 2 div 72 mul 5.25 72 mul translate
    depth ExpandKite

```

```
grestore

gsave
  13 golden sub 2 div 72 mul 5.25 72 mul translate
  depth ExpandDart
grestore
}
{
  printDart {
    gsave
    11 golden sub 2 div 72 mul 5.25 72 mul translate
    depth ExpandDart
    grestore
  } if

  printKite {
    gsave
    11 golden sub 2 div 72 mul 5.25 72 mul translate
    depth ExpandKite
    grestore
  } if

} ifelse

showpage
```

Appendix D

Colophon

This document was written in the \LaTeX document processing system with WinEdt 5.3 as the editor. Figures in the document were created with postscript and edited in Adobe Illustrator 8.0.

All the work was done in Windows XP environment on a computer with a Pentium 1.4GHz processor, 256MB of RAM and a 30GB disk drive. Such a device would cost about \$600 (monitor excluded) as of April, 2002.

Bibliography

- [AST⁺00] Eiji Abe, Koh Saitoh, H. Takakura, A. P. Tsai, P. J. Steinhardt, and H.-C. Jeong. Quasi-unit-cell model for an al-ni-co ideal quasicrystal based on clusters with broken tenfold symmetry. *Physical Review Letters*, May 2000.
- [Ber66] Robert Berger. The undecidability of the domino problem. *Memoirs of the American Mathematical Society*, 66, 1966.
- [BG97] C. Bandt and Petra Gummelt. Fractal Penrose tilings I: Construction and matching rules. *Aequationes Mathematicae*, 53:295–307, 1997.
- [BZ01] Duane A. Bailey and Feng Zhu. A sponge-like (almost) universal tile. 2001.
- [GKP94] Ronald L. Graham, Donald E. Knuth, and Oren Patashnik. *Fibonacci Numbers and Continuants*, chapter 6.6–6.7, pages 276–305. Addison-Wesley, Reading, second edition, 1994.
- [GS87] Branko Grünbaum and G. C. Shephard. *Tilings and Patterns*, chapter 10. W. H. Freeman and Company, New York, 1987.
- [Gum96] Petra Gummelt. Penrose tilings as coverings of congruent decagons. *Geometriae Dedicata*, 62(1):1–17, August 1996.
- [Hea00] Jason B. Healy. Automatic generation of Penrose empires. Technical report, Department of Computer Science, Williams College, 2000.
- [MRSZ97] Erich J. Muehlegger, Andrew S. Raich, Cesar E. Silva, and Wenhuan Zhao. Lightly mixing on dense algebras. *Real Analysis Exchange*, June 1997.

- [SBGC84] D. Shechtman, I. Blech, D. Gratias, and J.W. Cahn. Metallic phase with long-range orientational order and no translational symmetry. *Physical Review Letters*, 53:1951–1953, November 1984.
- [Sil02] Cesar E. Silva. *An Invitation to Ergodic Theory*. Preprint, 2002.
- [SS86] Joshua E. S. Socolar and Paul J. Steinhardt. Quasicrystals. II. unit-cell configurations. *Physical Review B*, 34(2):617–647, July 1986.